$2\pi^*$ resonance features in the electronic spectra of chemisorbed CO

B. Gumhalter and K. Wandelt
Institute of Physics of the University of Zagreb, YU-41001 Zagreb, Yugoslavia
and Fritz-Haber-Institut der Max-Planck-Gesellschaft, Faradayweg 4-6, D-1000 Berlin 33, West Germany

Ph. Avouris
IBM Thomas J. Watson Research Center, P.O. Box 218, Yorktown Heights, New York 10598
(Received 19 February 1987; revised manuscript received 14 September 1987)

The electronic spectra of CO chemisorbed on transition metals and copper as obtained with photoelectron spectroscopies, surface Penning spectroscopy, inverse photoemission spectroscopy, and x-ray absorption spectroscopy are discussed in regard to inherent features pointing to the existence of a CO $2\pi^*$-derived resonance in these adsorption systems. Since the various spectroscopies probe the CO-metal systems predominantly in the excited final state, the spectra of one and the same line, however, are also affected by differences in the dynamic relaxation processes and nonequilibrium final-state charge configurations which are specific to each particular experimental method. In order to arrive at a unified interpretation of some seemingly controversial features in the electronic spectra of chemisorbed CO, we have invoked the notion of the CO $2\pi^*$-*derived resonance*. Our model includes both initial-state chemical (i.e., backdonation-induced bonding) effects and final-state dynamical screening (relaxation) effects. Assuming a very small fractional occupation of the CO $2\pi^*$ resonance in the case of weak chemisorption systems (e.g., CO/Cu), and notably larger occupation in the case of strong chemisorption (e.g., CO/Ni), it is possible to give a *unified* interpretation of the experimental features such as the threshold energies, level shifts, line shapes, etc., observed with CO adsorbed on transition metals and copper. The great success of the concept of a resonance in interpreting these experimental spectral features as obtained with the various spectroscopies, provides, in turn, strong support for the actual existence of a CO $2\pi^*$-derived resonance in these adsorption systems.

I. INTRODUCTION

Adsorption of CO on Cu and transition metals has recently attracted an almost unprecedented attention of surface scientists, mainly because of the fact that it may be regarded as a prototype of nondissociative molecular chemisorption on metallic substrates. Since this type of adsorption has very many possible practical implications, extensive and systematic studies of CO adsorption have been undertaken. This has resulted in a huge number of publications which, in one way or another, deal with various physical and chemical aspects of adsorbed CO. However, despite the efforts made to interpret its characteristics, surprisingly little correlation has been established among the results obtained from different spectroscopies, implying that presently a unified model of the adsorbed CO spectral properties is still lacking.

This situation is particularly characteristic of the studies of the electronic spectra of chemisorbed CO. Here the experimental data are especially abundant, but the synthesis of various model descriptions which would emphasize their common features is still lacking. The present critical discussion aims at filling this gap by presenting a *unified* model for the interpretation of various spectral properties of adsorbed CO. In the following sections we review and analyze in the light of this model the experimental data obtained by a number of different spectroscopic methods. The underlying concept of our model description and the analyses of the measured spectra is a CO $2\pi^*$-derived valence-electronic resonance which is partially occupied by the charge backdonation from the substrate. As different spectroscopic techniques probe the adsorbates in different electronic final states, the experimental manifestation of the $2\pi^*$ resonance is necessarily both system *and* method specific. Hence, a distinction of its features requires detailed analyses of both initial- and final-state effects in the measured spectra.

The question of the existence and the manifestation of the $2\pi^*$-derived resonance in chemisorbed CO was first raised in the analyses of the ultraviolet photoemission spectra of adsorbed CO valence levels. Later, the question was augmented by the results obtained with other spectroscopic techniques. In our discussion we shall first point out the conceptual difficulties encountered in the attempts to interpret the adsorbed CO valence electronic spectra within the traditional molecular-orbital (MO) model of CO chemisorption. To overcome these apparent difficulties we propose the use of the $2\pi^*$ resonance model as an alternative. We shall pay special attention to the discussion of CO adsorption on Cu and Ni because these systems may be regarded as prototypes of weak and strong CO chemisorption, respectively. The main conclusion which derives from all our analyses and discussions is that the $2\pi^*$ resonance model provides a simple, yet complete and unified framework for a success-

ful interpretation of the features of the electronic spectra of chemisorbed CO such as level shifts and positions, threshold energies, line shapes and others.

II. ELECTRONIC LEVELS OF CHEMISORBED CO AND THE $2\pi^*$ RESONANCE MODEL

Early spectroscopic measurements of the electronic structure of CO adsorbed on metallic surfaces focused on the determination and the assignment of the outer or valence levels of the adsorbate. UPS (uv photoelectron spectroscopy) proved to be an almost ideal technique for this purpose due to its surface sensitivity and relatively high resolution. The UPS studies of CO adsorption on free-electron, noble, and transition metals revealed different types of interactions between the CO molecules and the metals concerned, a fact which was also reflected by the quite different values of the heat of adsorption of CO on these different substrates.

The UPS final-state relaxation shifts, of the 4σ-, 1π-, and 5σ- derived orbitals exhibited a unified behavior only for CO adsorption on Al,[1] Ag,[2] and Au,[3] and manifested themselves as about equal upward shifts (towards ε_F) for all three levels. These results indicated flat CO adsorption geometry and a purely physisorptive bonding mechanism in these systems.[4] On the other hand, in CO adsorbed on Cu and transition metals the shifts of the 4σ, 1π, and 5σ orbitals are not equivalent. UPS measurements revealed downward energy shifts of the 5σ level relative to the position of the other two levels, indicating thereby the presence of a specific initial-state interaction between the adsorbate 5σ and the substrate *s*-, *p*-, and *d*-band states. Since the mechanism of the CO interaction with metal atoms was already studied in the chemistry of carbonyls,[5,6] the bonding picture which was suggested by the analogy between the carbonyls and the CO adsorption complexes was that of charge donation of the adsorbate 5σ electrons to the substrate with a simultaneous charge backdonation from the substrate valence states into the $2\pi^*$-derived orbital of adsorbed CO. Recent calculations[7] for a variety of substrates modeled by metallic clusters of variable size have shown that the charge transfer into the $2\pi^*$-derived CO level indeed represents the major source of the adsorbate-metal cluster bond stabilization, although the $2\pi^*$ level of CO is itself antibonding in character and its occupation leads to a weakening of the oxygen-carbon bond.[8] Such calculations also confirm the experimentally found downward shifts of the 5σ derived level upon adsorption of CO on Cu,[9–14] and particularly on transition metals,[15–23] and that the 5σ level will be preferentially shifted to higher binding energy over the other valence CO levels even in the absence of the 5σ donation. This is because its charge centroid is closer to the surface and thus senses a higher value of the effective metal potential.[24] Additional information which could also be extracted from the angularly resolved UPS (e.g., Refs. 10, 19, 25, and 26) and complementary low-energy electron diffraction (LEED) measurements[27] was that CO adsorbed with the molecular axis perpendicular to the surfaces of most monocrystals, irrespective of the geometry of the adsorption site (on-top, hollow, or bridge position), or the strength of the chemisorptive bonding. [Exceptions are the systems CO/Ni(110) and CO/Pt(110) in which at full monolayer coverage and low temperatures the CO axis is 20° off normal.[25(a),25(b),28]

The backdonation-induced filling of the $2\pi^*$-derived levels in CO chemisorption on metals naturally raised the question regarding the observability and manifestation of this effect in various systems. This problem was also intimately connected with the nature of the $2\pi^*$-derived levels. Namely, in the traditional molecular orbital (MO) picture of CO chemisorption, two levels should derive from the strong hybridization between the $2\pi^*$ orbital (located about 1.5 eV above the vacuum level ε_V in free CO) and the substrate *d* band: a bonding one located below the substrate Fermi level ε_F, and hence occupied, and an empty antibonding one high above ε_F.[29] The former state should be detectable by UPS, but although some extra structure around ε_F has indeed been observed in various CO adsorption systems (Refs. 9 and 16), serious doubts have been expressed as to the assignment of this structure to a distinct MO-like $2\pi^*$-derived level.[19] A number of observations which contradict this picture have been reviewed and discussed.[29]

It is well known that the MO picture and the cluster models generally overestimate the roles of the *d* band in CO adsorption on noble and transition metals because they do not account for the *extended* structure of metallic *s,p* bands. It is also known from the Anderson-Newns model of chemisorption,[30] the calculations of atomic adsorption on jellium,[31,32] and embedded cluster calculations[33] that weak and moderately strong hybridization of adsorbate localized valence orbitals with broad substrate bands leads to a formation of *virtual bands of states* or *resonances* whose width depends on the strength of the adsorbate-substrate coupling. Such adsorbate-derived resonances or localized bands of states may be fractionally occupied by charge transfer from the substrate into the resonance states lying below the Fermi level of the system (see Fig. 1). If such a resonance forms upon CO adsorption on Cu and transition metals due to the hybridization of the CO $2\pi^*$ orbital with the substrate *s*, *p*, and *d* bands, two effects not accounted for by the conventional Blyholder model are expected.[34,35] First, even if the *center* of such a $2\pi^*$-derived resonance lies *above* ε_F, its wing may still extend below ε_F, allowing fractional charge transfer into the resonance (i.e., backdonation into the resonance); and second, the occupied and unoccupied parts of the resonance (which may be thought of as a fractionally occupied localized band of states) may become a source of intraresonance *dynamic* relaxation and polarization processes which are largely localized on the adsorbate.[34–38] These processes may affect, through the strong intramolecular interactions, all other adsorbate electronic levels and thereby modify their spectra independent of the spectroscopy employed.

Besides UPS, the occupied valence levels of chemisorbed CO have also been measured by surface Penning ionization electron spectrocopy (SPIES). This method enables one to disentangle the adsorbate-induced features from the valence electronic density of states of the underlying substrate. This property turns out particularly ad-

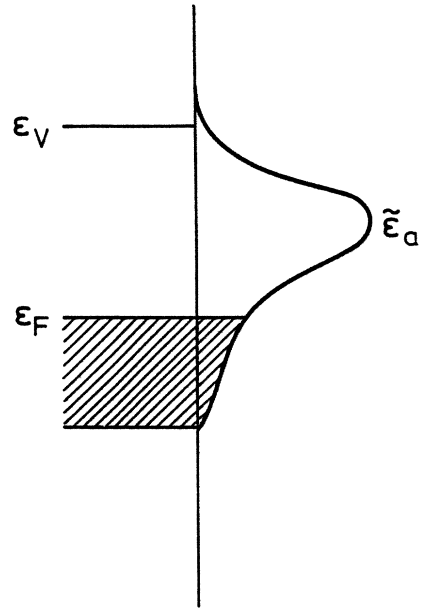

FIG. 1. Sketch of a simple adsorbate-induced resonance fractionally occupied by charge transfer from the substrate. $\tilde{\varepsilon}_a$ denotes the position of the resonance maximum here located above the Fermi level ε_F.

vantageous in the search of rather weak and relatively broad adsorbate valence electronic structures such as the occupied parts of the asserted CO $2\pi^*$ resonance which in UPS may be obscured by the strong emission from the substrate d bands. The occupied core levels of adsorbed CO have been studied by x-ray photoemission spectroscopy (XPS), the empty affinity levels by inverse photoemission spectroscopy (IPES) [or bremsstrahlung-isochromat spectroscopy (BIS)] and x-ray-induced intra-adsorbate core-to-valence electronic transitions [or near-edge x-ray-absorption fine-structure spectroscopy (NEXAFS)].

In all these and similar experiments carried out on adsorbed CO the measured spectra keep trace of the properties of the adsorbate initial electronic ground state and of the characteristics of various possible adsorbate final states. The latter, depending on the spectroscopic technique employed, may be ionized (UPS, SPIES, XPS, IPES) or excited neutral (NEXAFS). Since different final states are generally characterized by different relaxation effects, the extraction of the adsorbate chemical electronic structure from the measured spectra is difficult and often requires rather complicated analyses of the data. Despite this difficulty, however, the physical models of the true adsorbate ground-state electronic structure and of the associated relaxation mechanisms must satisfy the criterion of being able to interpret the manifestly different method-specific spectral features of the adsorption system at a unified footing. The analyses of the experimental data on CO adsorption on Cu and transition metals acquired by electron spectroscopies (UPS, SPIES, XPS), inverse photoemission, and adsorption spectroscopy, which are presented in Secs. III, IV, and V, respectively, demonstrate that the $2\pi^*$ resonance model satisfies this criterion.

III. $2\pi^*$ RESONANCE MANIFESTATION IN ELECTRON SPECTROSCOPIES

A. UPS

The adsorbate-induced spectral structures observed in the UPS-derived density of states of adsorbed CO below the Fermi level threshold have been interpreted by some authors[1–4,6–14,21] as a $2\pi^*$ spectral feature. However, in the majority of these assignments this feature has been associated with a MO-derived bonding level of energy $\varepsilon_{2\pi}^{MO}$ [cf. Ref. 29(b), Fig. 1], rather than with a structure reflecting only the occupied part of the resonance centered at $\tilde{\varepsilon}_{2\pi}$ *above* ε_F, and extending below ε_F. If the resonance picture of the CO adsorption, however, is adopted, some controversies in the CO/Cu and CO/Ni adsorption systems can be easily explained. In the systems CO/Ni(111) (Ref. 17) and CO/Ni(100) (Ref. 4) the CO-induced extra feature in the UPS difference spectrum appears *above* the Ni d-band bottom (cf. Fig. 2). This would be incompatible with the MO scheme in which the bonding level deriving from the hybridization of the CO $2\pi^*$ orbital with the substrate d-band would be likely to appear *below* the d-band bottom.[29] The same argument should apply to the CO/Cu systems (Fig. 3) in which the d band lies even between 2 and 4 eV below the Fermi level, i.e., completely below the $2\pi^*$-induced feature.

Because of the finite probing depth of UPS, the CO-related features are only superimposed on the metal valence-band emission, which in the case of the transition metals is very strong near ε_F. Therefore, any CO

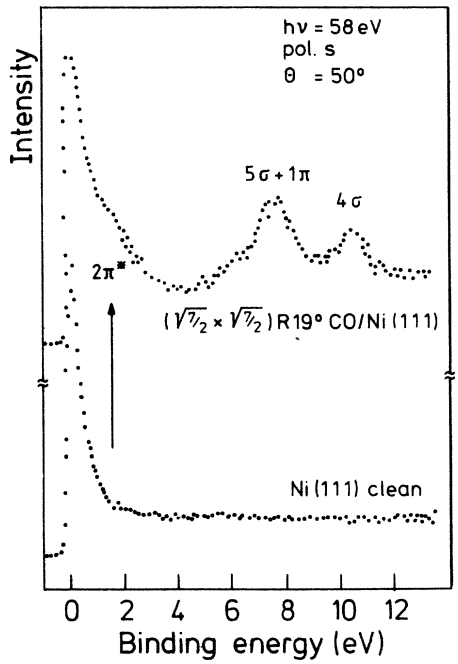

FIG. 2. Angular resolved valence-band spectra of clean and CO covered Ni(111) excited with synchrotron radiation of $\hbar\omega = 58$ eV and s polarization. Note the adsorption-induced extra emission from the partially filled CO $2\pi^*$ resonance. (From Ref. 17.)

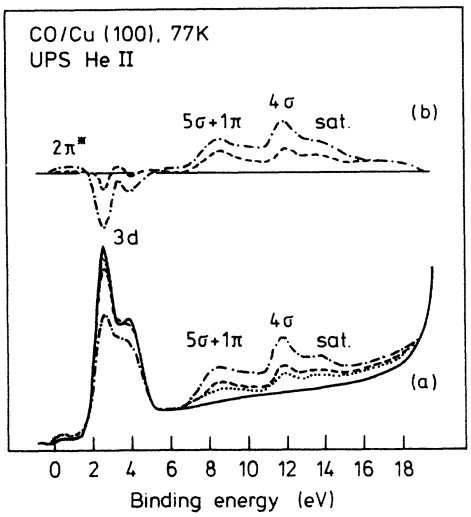

FIG. 3. (a) He II excited uv-photoemission spectra of CO adsorbed on Cu(100) at 77 K. ——, clean; · · · · and — — —, intermediate coverage; —·—·— saturation coverage. (b) Representative difference spectra (covered minus clean). (From Ref. 9.)

$2\pi^*$-related intensity manifests itself (if at all) only in difference spectra (CO covered minus bare metal spectrum). Such difference spectra, however, must be regarded with due reservation, because energy-dependent attenuation effects near ε_F owing to electron scattering in the adsorbate overlayer may also produce features in these difference spectra which could be misinterpreted as being characteristic of the electronic structure of the adsorbed CO-metal complex. But apart from the attenuation of the UPS difference spectra at ε_F encountered in all systems, the extra feature below ε_F observed in the systems CO/Ni and CO/Cu still exhibits the *shape* of an extending tail of a Lorentzian-like resonance centered above ε_F (cf. Figs. 2 and 3). This is rather important as it indicates the possibility of a partial filling of the resonance by charge transfer (see Fig. 1), in support of the backdonation mechanism.

B. Penning ionization

Although to a first approximation UPS spectra provide a rather direct replica of the density of states of adsorbed CO, their detailed analysis and assignment may be complicated by cross-section problems, overlapping peaks, etc. It took, for instance, several years until the problem of the correct identification of the strongly overlapping 5σ and 1π states of adsorbed CO could be solved by the use of angular and polarization-dependent UPS (e.g., Ref. 26). Even more problematic is a trustworthy assessment of the CO-induced $2\pi^*$-derived extra emission just below ε_F as pointed out above. These problems are absent in Penning electron spectroscopy of adsorbed CO.[39]

In Penning electron spectroscopy the adsorbate-covered surface is exposed to a beam of electronically excited, metastable He* atoms of thermal translational energy,[40] which serve as energy sources for electron emission characteristic of the adsorbate. This Penning ionization process is governed by an exchange mechanism[41] (Auger deexcitation), in which an electron transition from an adsorbate orbital into the 1*s* hole of the metastable He* is accompanied by emission of the excited 2*s* electron from the He.* The measured kinetic energy of the latter electron is determined by the relative energy separation of the He* 1*s* level and the adsorbate orbital concerned, and is therefore adsorbate specific. Since to a first approximation the rate of deexcitation is determined by the overlap of the He 1*s* wave function with the respective adsorbate orbital, this technique is extremely surface sensitive. In fact, in the case of an adsorbate-covered surface it is only sensitive to the outermost adsorbate orbitals with minimum interference by the electronic structure of the metal substrate underneath. This becomes evident from Fig. 4, which compares the Penning (^3S He*, ^1S He*) spectra with the UPS ($\hbar\omega = 21.2$ eV) spectrum of a CO-covered Cu(110) surface.[42] The Penning spectra exhibit only the CO 5σ-, 1π-, and 4σ derived signals, but no Cu(4*s*,*p* 3*d*) valence-band emission at all. This makes Penning spectroscopy particularly suited for studies of the CO-induced spectral changes just below ε_F of transition metals, isolated from the substrate valence-band emission. As an example Fig. 5 shows electron energy distributions from ^1S He* and ^3S He* excited Penning spectra of adsorbed CO near the Fermi level of Pd(111) and Cu(110).[42] The detection of appreciable electron emission in the energy interval between $\varepsilon_F = 0$ and 4 eV on Pd(111) is obvious, and has been detected for CO adsorbed on Ni(111) (Ref. 43) and potassium precovered Ni(111).[44] Since free CO has no occupied orbitals in this

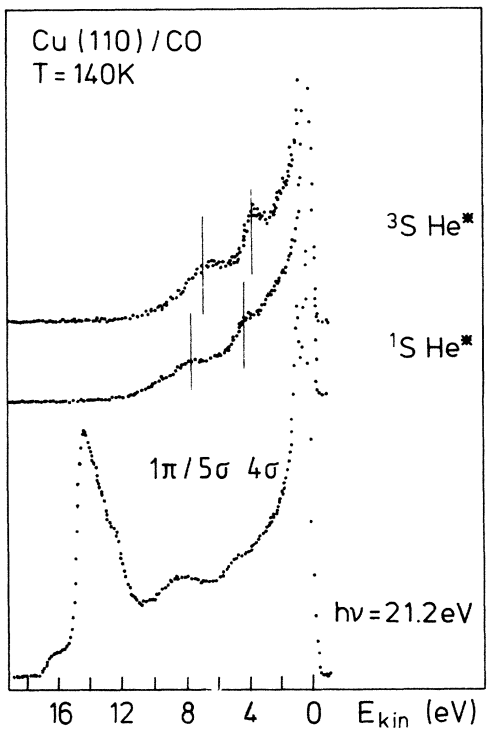

FIG. 4. UPS and Penning ionization (^1S and ^3S He*) spectra for CO adsorbed on Cu(110). (From Ref. 42.)

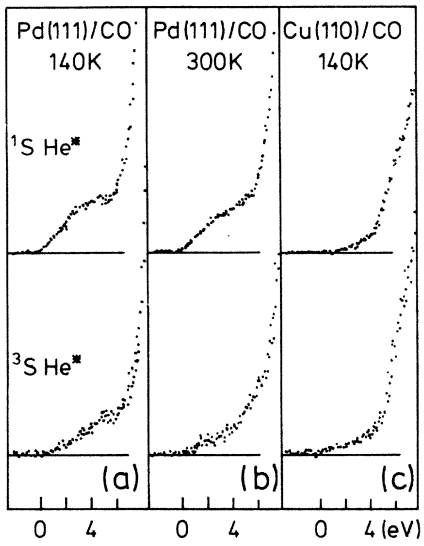

FIG. 5. Electron energy distributions from ^1S and ^3S He* excited Penning spectra of CO adsorbed on Pd(111) and Cu(110) near the Fermi level (from Ref. 42).

energy range it has been argued[42] that this emission may originate from the overlap with the wave functions which consist of a mixture of metal band and CO $2\pi^*$ states, hence of hybridized $2\pi^*$ resonance states. If this interpretation is correct[45] the emission between ε_F and 4 eV would correspond to the occupied tail of a $2\pi^*$-derived resonance of CO adsorbed on these transition metals and therefore would be the most direct evidence for the backdonation effect. Accordingly, with CO/Cu(110) the emission near ε_F is much weaker due to the reduced bonding strength and hence reduced degree of backdonation or $2\pi^*$ resonance occupation in this system.

C. XPS

As a consequence of a partial occupation of the $2\pi^*$ resonance, intraresonance excitations, although taking place in the valence region of the density of adsorbate states, would also strongly modify the XPS core spectra of adsorbed CO. In order to demonstrate this and make proper contact with the experimental evidence and other spectroscopies, we shall make use of the model introduced in Refs. 36 and 46, which proved very useful for the description of dynamic screening and relaxation properties of adsorbates.[38,46–49] The model is based on an extension of the original Anderson-Newns model Hamiltonian of chemisorption[30(a)] in which the adsorbate $2\pi^*$ valence states with respect to CO-metal interaction are denoted by $|m,\sigma\rangle$ where $m=\pm1$ and $\sigma=\pm\frac{1}{2}$ are the components of the angular momentum and spin of an electron in the doubly degenerate CO $2\pi^*$ orbital, respectively. This model takes into account both the hybridization of the $2\pi^*$ valence states $|m,\sigma\rangle$ of the adsorbate with the substrate valence band states $|k,\sigma\rangle$, and the coupling of the adsorbate valence states $|m,\sigma\rangle$ and adsorbate core states $|1s,\sigma\rangle$ with the surface polarization field. The latter may conveniently be described within the linear-response formalism using the properties of the surface response function.[38,50] In the second quantization, the Hamiltonian of the composite system may be written in the form:[47]

$$H=\sum_{k,\sigma}\varepsilon_k n_{k\sigma}+\sum_{\sigma}\varepsilon^0_{1s}n_{1s\sigma}+\sum_{m\sigma}\varepsilon_{m\sigma}n_{m\sigma}+\sum_{k,m,\sigma}(V_{mk}c^\dagger_{m\sigma}c_{k\sigma}+\text{H.c.})+\sum_{m,\sigma,m',\sigma'}U_{m\sigma,m'\sigma'}n_{m\sigma}n_{m'\sigma'}+\sum_{Q}\hbar\omega_Q a^\dagger_Q a_Q$$
$$+\sum_{m,\sigma}n_{m\sigma}\sum_{Q}\lambda^m_Q(a^\dagger_Q+a_{-Q})-\sum_{\sigma}(1-n_{1s\sigma})\sum_{Q}\lambda^s_Q(a^\dagger_Q+a_{-Q})-\sum_{m,\sigma}U_{1s\sigma,m\sigma}n_{m\sigma}(1-n_{1s\sigma})\,. \quad (1)$$

The first three terms on the right-hand side of Eq. (1) describe the unperturbed states of the substrate ($|k,\sigma\rangle$) and the adsorbate ($|m,\sigma\rangle$ and $|1s,\sigma\rangle$), of unperturbed energy ε_k, ε^0_{1s} and $\varepsilon_{m\sigma}$, respectively, where $n_{k\sigma}=c^\dagger_{k\sigma}c_{k\sigma}$, $n_{1s\sigma}=c^\dagger_{1s\sigma}c_{1s\sigma}$, and $n_{m\sigma}=c^\dagger_{m\sigma}c_{m\sigma}$ are the corresponding electron number operators expressed through the electron creation and annihilation operators $c^\dagger$ and c, respectively. The fourth term describes the hybridization between the adsorbate $2\pi^*$ orbital and the substrate s,p band, which gives rise to the broadening of the $2\pi^*$-derived level into a resonance of full width at half maximum (FWHM) $\Gamma^0_{2\pi}$. The fifth term describes two-body intraorbital interactions among the electrons occupying the $2\pi^*$-derived states. The next three terms describe the screening field of the substrate and the interaction of the electron and hole charge in the $2\pi^*$ and $1s$ core levels, respectively, with the screening field (i.e., the linear surface response of the substrate charge-density fluctuations) through the corresponding coupling matrix elements λ_Q. Here Q are the quantum numbers of the elementary excitations of energy $\hbar\omega_Q$ characteristic of the substrate surface response and $a^\dagger_Q$ and a_Q are the corresponding creation and annihilation operators, respectively. Of particular importance is the last term in Eq. (1) which describes the intra-adsorbate relaxation process subsequent to the core-hole creation. The sudden appearance of the uncompensated charge of the core hole pulls down the energy of all the outer adsorbate orbitals by the amount of an intra-adsorbate Coulomb attraction U. Hence the valence states within the CO $2\pi^*$-derived resonances will be shifted down by the core-hole potential described by $U_{1s\sigma,m\sigma}$, hereafter frequently abbreviated as $U_{1s,2\pi}$, and this intra-adsorbate relaxation event will be followed by an interplay of three *dynamic* screening processes: (i) extra-adsorbate screening of the core hole by the surface response of the substrate[38,50] [described by the core-hole coupling to the polarization field in Eq. (1)]; (ii) excitation of electron-hole pairs within the resonance or intraresonance charge-density fluctuations;[36,37] and (iii) charge transfer (or electron resonance tunneling) from the substrate into those adsorbate resonance states which have been pulled below ε_F by switching on the core-hole po-

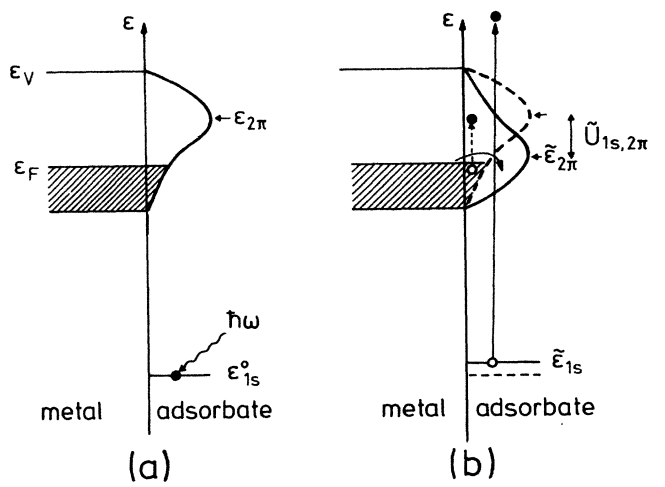

FIG. 6. Energetics of the adsorbate valence resonance and core levels in XPS. (a) initial state, (b) final state with core hole and the interaction $\tilde{U}_{1s,2\pi}$ switched on. Empty resonance states pulled below ε_F are filled by charge transfer from the substrate. Intraresonance shakeup excitation is denoted by a vertical dashed arrow.

tential $U_{1s\sigma,m\sigma}$.[36,37,51(a)] The physics of these processes (cf. Fig. 6) has been discussed at length in Refs. 36–38, 47, and 51, and here we shall only outline its implications on the shapes and shifts of the XPS core-hole spectra of chemisorbed CO. The screening processes (i)–(iii) all contribute to an upward relaxation shift of the adsorbate core-hole energy, from the gas-phase value ε^0_{1s} to the fully relaxed value $\bar{\varepsilon}_{1s}$. The latter energy when referenced to the Fermi level of the substrate, is usually termed as the threshold energy. Quite generally, the core-level relaxation shift as observed in XPS will comprise an extra-adsorbate (polarization or image) contribution v_{1s} due to the interaction of the hole with its image,[38,51(b)] and a chemically induced contribution $\Delta\varepsilon_{\rm chem}$ deriving from the change in the occupation of the resonance in the initial and final state[38] induced by switching on of the interaction $U_{1s\sigma,m\sigma}$. Within the model described by Eq. 1 these shifts read[47]

$$v_{1s}=\sum_{\rm Q}(\lambda^s_{\rm Q})^2/\hbar\omega_{\rm Q}\ , \tag{2}$$

and

$$\Delta\varepsilon_{\rm chem}=-\sum_{m,\sigma}\int_{-\infty}^{\varepsilon_F}\frac{\delta_{m\sigma}(\varepsilon)}{\pi}d\varepsilon\ . \tag{3}$$

Here $\delta_{m\sigma}(\varepsilon)$ is the effective phase shift for a single electron scattering off the 1s core hole in the (m,σ)th channel of the adsorbate valence resonance:[47]

$$\delta_{m\sigma}(\varepsilon)=\arctan\left[\frac{\pi\rho^0_{m\sigma}(\varepsilon)\tilde{U}_{1s,m\sigma}}{1+\tilde{U}_{1s,m\sigma}y_{m\sigma}(\varepsilon)}\right]\ , \tag{4}$$

where $\rho^0_{m\sigma}(\varepsilon)$ is the effective one-electron density of states characterizing the (m,σ)th component of the $2\pi^*$ derived resonance *before* the creation of the core hole in the 1s state, $y_{m\sigma}(\varepsilon)$ is its Hilbert transform, $\tilde{U}_{1s,m\sigma}$ is the *screened* core-hole potential

$$\tilde{U}_{1s,m\sigma}=U_{1s,m\sigma}-2v_{1s\text{-}2\pi}\ , \tag{5}$$

and $v_{1s\text{-}2\pi}$ is the interaction between the $2\pi^*$ electron with the image of the core hole. The XPS core-level threshold energy with respect to ε_V will thus be given by

$$\bar{\varepsilon}_{1s}=\varepsilon^0_{1s}+v_{1s}-\Delta\varepsilon_{\rm chem}\ . \tag{6}$$

Here it is important to notice that in the absence of the resonance broadening of the $2\pi^*$-derived level in the initial and final state (i.e., before and after the core-hole creation), the term (3) would be either zero or would give rise to the complete screening of the core hole depending on whether the $2\pi^*$ level remains above or is pulled below ε_F in the final state. In the former case the relaxation and screening of the core hole will proceed only through the extra-adsorbate mechanism (i), i.e., extra-adsorbate dynamic image screening. This seems to be the situation in the UPS spectra of CO condensed on Al,[1] Ag,[2] and Au.[3] In the chemisorption case, v_{1s} may be reduced due to the larger role which the local or intra-adsorbate screening through the charge transfer may play [mechanism (iii)].

The XPS core-level spectra of chemisorbed CO may exhibit complicated structure which differs substantially from the single peak characteristic of free CO. Beyond Eq. (6) the resonance model can also fully explain these nontrivial shapes of the spectra by studying the *time dependence* of the mechanisms (i)–(iii) embodied in the Hamiltonian (1).

We shall first consider the case of CO adsorption on a Ni(111) surface, which, although being an example of strong CO chemisorption, can be more easily interpreted as regards the shape of the core spectra. The O 1s and C 1s peaks of the CO/Ni(111) system exhibit an *asymmetric* Lorentzian-like structure located at the threshold energy $\bar{\varepsilon}_{1s}$ [cf. Fig. 7 (Ref. 17)]. The experimental core level threshold energies [Eq. (6)] for the CO/Ni(111) system determined from these spectra are

$$\bar{\varepsilon}^{\,F}_{\rm C\ 1s}=285.3\ {\rm eV},\quad \bar{\varepsilon}^{\,F}_{\rm O\ 1s}=531.0\ {\rm eV}\quad [{\rm CO/Ni(111)}] \tag{7}$$

(relative to the Fermi level). The asymmetry of the peaks is interpreted as a manifestation of the Anderson orthogonality theorem[52] or the infrared-threshold divergence[53] in the adsorbate core spectrum which occurs due to the multiple emission of low-energy intra-resonance electron-hole pairs (shake-up processes), excited by the sudden (transient) switching on of the core hole potential $U_{1s,2\pi}$ in x-ray photoemission (cf. Fig. 6). In the absence of the broadening of the core level by the finite hole lifetime, the XPS core-level spectrum $\rho_{1s}(\varepsilon)$ would be described by an integrable, totally asymmetric infrared threshold divergence:[36,37,47]

$$\rho_{1s}(\varepsilon)\propto\Theta(\bar{\varepsilon}_{1s}-\varepsilon)/(\bar{\varepsilon}_{1s}-\varepsilon)^{\alpha}\ \text{as}\ \varepsilon\to\bar{\varepsilon}_{1s}\ , \tag{8}$$

where Θ is the unit step function and the critical exponent α is given by

$$\alpha=1-\sum_{m,\sigma}n^2_{m\sigma}\ , \tag{9}$$

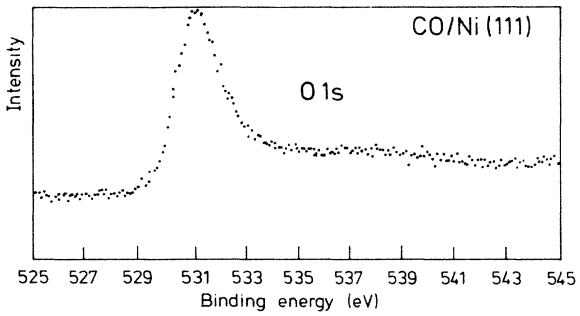

FIG. 7. XPS oxygen 1s core-level spectrum for CO/Ni(111) (From Ref. 17.)

and $n_{m\sigma}$ is the number of extra electrons brought into the scattering channel (m,σ) of the resonance to screen out the core hole. This number is given by the Friedel rule

$$n_{m\sigma}=\delta_{m\sigma}(\varepsilon_F)/\pi \ . \tag{10}$$

Since the critical exponent α depends on the initial resonance density of states at the Fermi level through Eqs. (4), (9), and (10), it is obvious that a pronounced asymmetry of the core-level threshold peaks in chemisorbed CO may therefore provide experimental evidence for the existence of a finite $2\pi^*$ resonance density of states at ε_F and the relaxation processes emerging thereof. In real systems the finite lifetime of the core level will act to round off the threshold divergences [Eq. (7)] into skew Lorentzians, but the asymmetry of the threshold peak will always persist.[37] This has indeed been observed for a variety of chemisorbed adsorbates[38,54,55] and *other* mechanisms which could give rise to the same effect have been *carefully eliminated* in these experiments to avoid interpretational ambiguities.[54] Only the extra-adsorbate electron-hole emission within the substrate conduction band (dynamic image screening) could produce a similar effect.[50] However, for chemisorption systems the coupling constant pertinent to this mechanism (essentially the effective value of λ_Q/ω_Q) is estimated to be weaker than the coupling constants $\tilde{U}_{1s\sigma,m\sigma}\rho^0_{m\sigma}(\varepsilon_F)$ which determine $\delta_{m\sigma}$ [Eq. (4)] and are responsible for intraresonance excitations. This coupling strength reduction occurs due to the screening of the core hole by the charge transfer onto the adsorbate[36,51(a),56] in the final relaxed state.

The present interpretation of a rather simple shape of the XPS 1s core-level spectra of CO/Ni(111) in terms of the $2\pi^*$ resonance model is straightforward, but the systems CO/Ni(100) (Ref. 16) and CO/Cu(100),[9] which exhibit more complicated XPS core spectral structure, require a more refined treatment. Nonetheless, their interpretation is also possible within the resonance picture and the model described by Eq. (1). To demonstrate this we first note that the strength of the CO-metal chemisorption bond decreases as one goes from CO/Ni(111) to CO/Cu(100), the latter system being already an example of weak chemisorption. It has been shown using a simpler and spinless (nondegenerate) version of the Hamiltonian (1) that in relatively weak chemisorption systems the adsorbate core spectra may exhibit a double-peak structure with maxima at the threshold [Eq. (6)] and an unrelaxed energy below the threshold[48] (i.e., at the higher-binding-energy side from the threshold). The relative weights of these peaks depend on the strength of the core-hole potential $\tilde{U}_{1s,2\pi}$ and on the hybridization matrix element V_{km} (and *a fortiori* on the resonance width $\Gamma^0_{2\pi}$ in the initial state). Thus, in the limit $\tilde{U}_{1s,2\pi}/\Gamma^0_{2\pi}<1$ the majority of the spectral weight will be concentrated at the threshold peak (case of strong chemisorption), whereas in the opposite case $\tilde{U}_{1s,2\pi}/\Gamma^0_{2\pi}>1$, which is the atomic or molecular limit of the present many-body problem, most of the spectral weight will be concentrated in the unrelaxed peak. In the intermediate regime $\tilde{U}_{1s,2\pi}\sim\Gamma^0_{2\pi}$ one may expect a double-peak structure or shoulders accompanying the peaks of dominant intensity. A shoulder at the high-binding-energy side of the threshold O1s and C1s peaks has been found in the system CO/Ni(100),[16] which is a weaker chemisorption system than CO/Ni(111). First-principles cluster calculations[16] have readily predicted a double-peak XPS core-hole spectrum in this system although here the $2\pi^*$ *resonance* existence has not been invoked explicitly. Hence, the information emerging from these calculations is restricted only to the peak separation and their relative intensities, and not to the overall shape of the spectra. A two-peak structure consisting of a strong asymmetric threshold peak and a weak satellite has also been detected for one single CO adsorption state on W(110),[54,55] the former feature signifying the presence of a fractionally occupied $2\pi^*$ resonance in the initial state of the adsorbate.

The structure of the XPS core-level spectra becomes even more complicated in CO adsorption on Cu. A

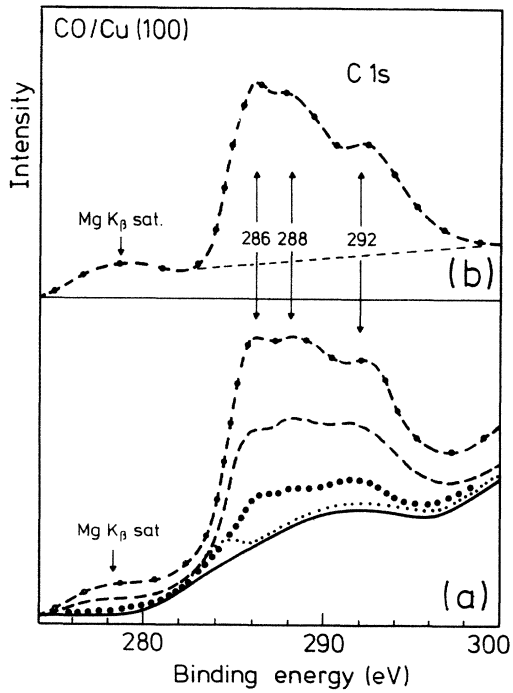

FIG. 8. (a) Carbon 1s core-level spectrum from CO adsorbed on Cu(100). ——, clean; · · · ·, and — — —, intermediate coverages; – – –, saturation coverage. Each trace represents the average of four spectra. (b) Difference spectrum (covered minus clean) at saturation coverage. (From Ref. 9.)

triple-peak C 1s spectrum in CO/Cu(100) has been observed[9] (cf. Fig. 8), with the threshold at

$$\tilde{\varepsilon}^{F}_{C\,1s}=286 \text{ eV} \quad [\text{CO/Cu}(100)] \tag{11}$$

relative to the Fermi level, and such features were later also detected with CO adsorbed on polycrystalline Cu.[11] The occurrence of the third peak between the one at the threshold and the one at the unrelaxed energy could be interpreted as due to the hybridization of the $2\pi^*$ orbital of CO with the peculiar band structure of Cu, viz., a broad s,p band and a rather narrow d band located 2 eV below the substrate Fermi level.[57] Again as in the former cases, the notation of the $2\pi^*$-derived resonance was invoked to interpret successfully the experimental data. Of course, such a statement may also be inverted so as to read that the shapes of the XPS core-level spectra of adsorbed CO give indirect evidence for the existence of the $2\pi^*$-derived resonance in the systems investigated. Direct evidence, however, could only be obtained from spectroscopies which measure the unoccupied, i.e., the dominant part, of the $2\pi^*$ resonance density of states directly. This is the case in inverse photoemission (IPES or BIS) and x-ray absorption or x-ray-induced core-to-valence excitation spectroscopy.

IV. $2\pi^*$ RESONANCE MANIFESTATION IN INVERSE PHOTOEMISSION

Since the evidence available from the UPS, Penning, and XPS studies of chemisorbed CO indicate that the $2\pi^*$-derived resonances may be rather broad and centered above ε_F of the respective substrates, a clear evidence for the existence of the $2\pi^*$ resonance could be obtained by measuring the resonance density of states above the Fermi level. Such measurements can be carried out by inducing electronic transitions into the unoccupied part of the resonance above ε_F, and currently three methods which make use of this principle are employed: electron energy-loss spectroscopy (EELS), inverse photoemission (IPES or BIS), and x-ray-induced core-to-valence transitions [NEXAFS or XANES (x-ray absorption near-edge structure)]. The latter two methods, which have been applied to the studies of CO chemisorption only recently, have provided rather direct evidence on the $2\pi^*$ resonance features in the measured spectra.

In IPES electrons make radiative transitions from a free, itinerant state into a localized adsorbate state above ε_F. The experiments can be carried out in two ways. Experimentally easier is to vary the energy of the incoming electrons and to detect the intensity of the emitted photons of fixed energy, e.g., 9.3 eV, with a simple Geiger-Müller detector.[58] More involved is it to measure the intensity *and* energy of the emitted photons at fixed primary electron energy using a monochromator.[59] For a fixed energy of the incoming electron, the energy and the intensity of the photons emitted in the transitions give a direct measure of the density of final adsorbate electronic states of the system with $N+1$ electrons. The final electron state derives from an unoccupied initial state of the system of N electrons and in this regard IPES represents a time-reversed process relative to direct photoemission.[60] However, the energetics of the final states as revealed by IPES will reflect the features of an $(N+1)$-electron system which may differ from those of the N-electron system. If the addition of an extra electron does not perturb much the levels of an N-electron system, as in the case of delocalized electronic states in the bands of solids or strongly interacting overlayers, the density of the final electronic state will be practically identical to the density of the initial unoccupied state. In isolated or not strongly interacting adsorbates, however, these levels comprise localized states or localized bands of states, and the situation is different because of the presence of strong local many-body interactions which accompany the transition of the IPES electron into a localized adsorbate state. The transient switching-on of the localized interactions will give rise to the occurrence of relaxation shifts and a modification of the spectral shapes of the adsorbate levels probed by IPES.

In the photoemission spectra of adsorbates (both UPS and XPS), one observes an upward relaxation shift of the initially occupied levels [cf. Eq. (6)]. In order to emphasize the difference between the relaxation shifts in the electron spectroscopies and inverse photoemission, we first note that in the former case the shift is defined as the difference between the corresponding one-electron Koopmans value and the true final-state relaxed energy. The difference occurs because the system has made a transition from a neutral N-electron state to a positively ionized $(N-1)$-electron state characterized by a different final-state interaction which perturbs the electrons (interaction between the photoinduced hole and its image). Schematically, this can be demonstrated as follows. Denoting by zero the ground-state energy of the N-electron system, the total energy of the initial photoemission state is $E_i=\hbar\omega$, where $\hbar\omega$ is the photon energy. The final photoemission state of total energy E_f is characterized by the kinetic energy of the photoelectron ε_p and of the hole in the adsorbate state $|a\rangle$ (formerly occupied) with energy $-\varepsilon_a^0$, shifted by the hole-image attraction $-v_a$ where $v_a>0$. The energy balance $E_i=E_f$ then gives

$$\hbar\omega=\varepsilon_p-(\varepsilon_a^0+v_a)=\varepsilon_p-\tilde{\varepsilon}_a\ , \tag{12}$$

i.e., the photoemission relaxation shift of an adsorbate level is *upward,* in full accordance with the microscopic model [Eqs. (1) and (6)].

The above simple analysis of the relaxation shifts of the adsorbate-occupied levels solely in terms of image interactions applies only to physisorbed adsorbates, and not to CO chemisorbed on Cu and transition metals. However, despite its simplicity, it provides a good interpretation of the valence-level relaxation shifts for CO physisorbed on Ag. In this case the molecular axis lies parallel to the surface, and the UPS measurements on the CO/Ag(110) system have indeed revealed an *upward* relaxation shift of 0.7 eV for all three occupied valence orbitals 4σ, 1π, and 5σ.[2(b)]

On the other hand, in IPES the adsorption system makes a transition from a neutral N-electron state to an $(N+1)$-electron state, again characterized by charge nonequilibrium and hence different final-state energetics. Here the initial IPES state of the system is characterized

by the energy of the IPES electron ε_p, whereas in the final state the electron energy is $\varepsilon_b^0 - v_b$, where ε_b^0 is the energy of the formerly unoccupied adsorbate state $|b\rangle$, and v_b is the electron-image attraction, and a photon of energy $\hbar\omega$ is emitted. The energy balance now gives

$$\hbar\omega = \varepsilon_p - (\varepsilon_b^0 - v_b) = \varepsilon_p - \bar{\varepsilon}_b \ , \tag{13}$$

i.e., the relaxation shift of the adsorbate levels in IPES is *downward,* in contrast to direct photoemission.

In electron scattering from free CO the external electron may be caught into the affinity level which is a virtual localized state of energy about 1.8 eV above the vacuum level ε_V. The EELS measurements carried out on the CO/Ag(110) physisorption system reveal a *downward* relaxation shift of the $2\pi^*$ affinity level by about 0.6 eV relative to the gas-phase value.[2(c)] This is again in complete accordance with the above simple analysis and the UPS measurements since with flat adsorption geometry the centroids of the charge in all CO orbitals should be equally separated from the surface, giving rise to image shifts of approximately the same magnitude. When the CO molecule is brought to the surface of Cu and transition metals, the features of the affinity level will be changed by the hybridization term V_{km} in Eq. (1) which will give rise to chemical or initial-state effects, in addition to two final-state interactions present only after the transition of the system from the neutral N-electron state to the ionized $N+1$ electron state. In the latter state the interactions λ_Q^m and $U_{m\sigma,m'\sigma'}$ are switched on because they are proportional to the electronic densities in the m states (i.e., $2\pi^*$ states) and hence will be responsible for the final-state relaxation shifts of the affinity level. However, due to the upright adsorption geometry in these systems even the relaxation shifts of the nonbonding orbitals will depend also on their separation from the surface.

A. Weak chemisorption: CO/Cu

Two CO/Cu systems have been studied by inverse photoemission, namely CO/Cu(110) (Ref. 61) and CO/Cu(100).[62] According to their relatively low heat of adsorption, both can be regarded as weak chemisorption systems in which CO adsorbs perpendicular to the surface. In CO/Cu(110) inverse photoemission revealed the existence of a single *asymmetric* peak located 0.9 eV below the vacuum level (i.e., 3.4 eV above ε_F) with half-width varying from 1.9 to 2.6 eV as a function of increasing coverage (see Fig. 9). The peak was interpreted as a BIS spectrum of the $2\pi^*$ derived resonance of the adsorbate. Since in the present system the CO overlayer is disordered, in particular the low-coverage spectrum is, in fact, most representative of the substrate-induced effects on the shape of the CO $2\pi^*$ resonance. In order to interpret these spectral features theoretically[63] one can assume hybridization between the CO $2\pi^*$ orbital and the substrate s,p bands and make use of the fact that the screening properties of the Cu surface can, to a good approximation, be represented by those of a free-electron metal. By using Eq. (2), with λ_Q^m instead of λ_Q^s,[63] it is possible to calculate the downward final-state screening relaxation shift

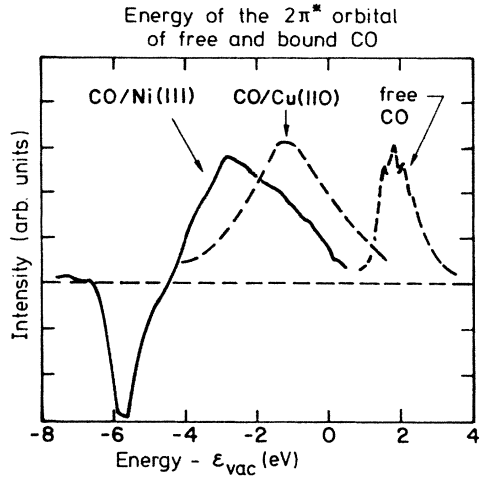

FIG. 9. IPE difference spectrum (covered minus clean) for CO adsorbed on Cu(110) at maximum coverage (Ref. 61) and on Ni(111) at $\frac{1}{3}$ monolayer coverage [Ref. 66(b)].

$$v_{2\pi}^0 = 3.1 \text{ eV} \tag{14}$$

for a *static* electron residing in the $2\pi^*$ orbital of CO adsorbed on Cu. Hence, $v_{2\pi}^0$ is an upper bound for the magnitude of the true relaxation shift $v_{2\pi}$ of an electron in the *hybridization-broadened* $2\pi^*$-derived orbital of the present adsorption complex.

The asymmetric broadening of the $2\pi^*$-derived resonance can be explained and calculated by treating the seventh term on the right-hand side of Eq. (1) as a transient perturbation and neglecting the intraorbital correlation $U_{m\sigma,m'\sigma'}$ due to the negligible initial-state occupation of the resonance

$$N_{2\pi} = \sum_{m,\sigma} n_{m\sigma} \tag{15}$$

because of the large separation between the resonance center and ε_F in the initial state (i.e., $\Gamma_{2\pi}^0 < \bar{\varepsilon}_{2\pi} - \varepsilon_F$ even in the final state). Namely, finite $U_{m\sigma,m'\sigma}$ and $N_{2\pi}$ can lead to a new charge-transfer screening mechanism in IPES which would be similar to that in XPS, but with the direction of the charge transfer reversed, i.e., from the adsorbate to the metal.[64] However, although this mechanism can operate on other adsorbates with valence levels near ε_F, it is not expected to be important in the case of CO.[29(a)] The asymmetric shape of the $2\pi^*$-derived state observed in IPES can within the present model be explained by the nonadiabatic screening [through the substrate low-energy (soft) electron hole pairs] of the IPES electron suddenly promoted into the resonant state. The line shape of the bare $2\pi^*$ resonance in each (m,σ) channel in the absence of nonadiabatic screening is described here by a Lorentzian-like structure of bare FWHM

$$\Gamma_{2\pi}^0(\varepsilon_{2\pi}^0 - v_{2\pi} - \Lambda_{2\pi}) \ ,$$

where

$$\Gamma_{2\pi}^0(\varepsilon) = 2\pi \sum_k |V_{km}|^2 \delta(\varepsilon - \varepsilon_k) \ , \tag{16a}$$

$$\Lambda_{2\pi} = \Lambda_{2\pi}^0(\varepsilon_{2\pi}^0 - v_{2\pi}) \tag{16b}$$

and $\Lambda^0_{2\pi}(\varepsilon)$ is the chemical level shift of the resonance [obtained as the Hilbert transform of $\Gamma^0_{2\pi}(\varepsilon)$].[30] The soft e-h pair component of image screening, although contributing little to the image shift $v_{2\pi}$ of the $2\pi^*$ level, will modify strongly the IPES spectrum from a symmetric peak of bare width $\Gamma^0_{2\pi}$ to an asymmetric one of larger effective width $\Gamma_{2\pi}$.[63] The latter shape shows up experimentally and represents an interplay between the mechanism of hybridization (chemical effect) and nonadiabatic screening (dynamical polarization effect).

The interplay between the hybridization of the $2\pi^*$ orbital with the metal and the substrate image screening will also affect the magnitude of the true image shift $v_{2\pi}$ of the resonance. The interference between the substrate-induced dynamic screening and the resonant tunneling leading to the delocalization of the $2\pi^*$ electrons will give rise to a reduction of the screening shift within the resonance from the value $v^0_{2\pi}$ to

$$v_{2\pi}=v^0_{2\pi}+\Delta v^0_{2\pi} , \tag{17a}$$

where[69]

$$\Delta v^0_{2\pi}=-\left[2\frac{v^0_{2\pi}}{\hbar\omega_s}\Lambda-v^0_{2\pi}\Lambda'\right] . \tag{17b}$$

Here $\hbar\omega_s$ is the surface plasmon energy characteristic of the substrate and

$$\Lambda'=\partial\Lambda(\varepsilon^0_{2\pi}-v^0_{2\pi})/\partial\varepsilon\simeq(\Gamma^0_{2\pi}/W_{sp}) ,$$

where W_{sp} is the substrate s,p band width. Since the latter quantity is usually large, $\Delta v^0_{2\pi}$ will be dominated by the first term in the bracket on the right-hand side of Eq. (17b), provided the chemical shift in the system considered is not negligible.

Two conclusions concerning the adsorbed CO $2\pi^*$ spectral shapes emerge from the above discussion. First, the $2\pi^*$-level IPES spectra are affected by the substrate dynamical image screening which shifts the level downward below ε_V, and second, the nonadiabatic screening contributes to the broadening of the IPES spectra by an amount of the order of 1 eV. However, although this final-state broadening is a significant effect,[63] it cannot explain the *complete* width of the observed $2\pi^*$ peak in the CO/Cu(110) IPES spectrum. Therefore, chemically induced or *initial-state* broadening of the $2\pi^*$-derived level due to resonance tunneling *must be* invoked in order to interpret the IPES data, and this fact may be regarded as a *direct evidence* for the existence of the $2\pi^*$-derived *resonance* in the CO/Cu(110) system.

The IPES studies of the CO/Cu(100) system[62] showed two peaks separated by 1 eV and centered at 1.1 eV below ε_V. The FWHM of both peaks was about 1.7 eV, not large enough relative to the peak separation to make their resolution as distinct features impossible. Since CO/Cu(100) is an ordered system additional broadening of IPES peaks may be expected due to dispersion effects. Cluster calculations for a single adsorbed CO molecule suggest[62] that the observed peaks represent the capture of the electron in a bonding and an antibonding level formed by the hybridization of the CO $2\pi^*$ level with the metal p_π levels. Of course, finite cluster calculations do not provide information on the peak widths, but the same arguments as outlined above for the disordered CO/Cu(110) system should hold here as well. The final-state dynamic screening effects should here broaden the spectra by almost an equivalent amount, but this broadening, as before, cannot explain the observed total width of the peaks. Hence, the resonance broadening must again be present as an *initial*-state effect. This is also strongly supported by the observed difference in the widths of the peaks in CO/Cu(100) and CO/Cu(111) adsorption systems.[62] The latter system is characterized by a hybridization gap extending from ε_F to ε_F+4 eV. Lastly, it should be pointed out that recent calculations[65] indicate that *vibronic* effects may also make a significant contribution to the IPES width of the $2\pi^*$-derived levels of adsorbed CO.

B. Strong chemisorption: CO/Ni

$2\pi^*$ resonances of even larger width and located farther below ε_V have been observed for CO adsorbed on transition metals Ni,[66] Pd,[67] and Pt.[68] In these systems the interpretational difficulties become more serious because of the more complicated electronic structure of the underlying substrates. However, the same qualitative conclusions regarding the existence of the resonance should hold in these cases as well.

In the system CO/Ni(111) it has been found[66] by analyzing the IPES difference spectra that the lowest empty virtual state of the adsorbate is centered between 3.5 and 3 eV above ε_F and exhibits a FWHM of about 4 eV at the coverage of $\frac{1}{3}$ monolayer (see Fig. 9). This spectral feature has been interpreted as a $2\pi^*$-derived resonance which is pulled 2.5 eV below ε_V due to the combined effect of substrate image screening and hybridization of the $2\pi^*$ orbital of CO with the substrate $4s,p$ bands.[66] The magnitude of the image screening shift $v_{2\pi}$ depends again on the degree of the delocalization of the $2\pi^*$ IPES electron. If the localization in the system CO/Ni(111) were about the same as in the weak chemisorption system CO/Cu, one might expect $v_{2\pi}$ for CO/Ni to be of the same order as for CO/Cu, for similar adsorption geometry. This is so because the surface response functions which determine the bare relaxation shifts $v^0_{2\pi}$ satisfy universal sum rules for all metals.[38] However, since the chemical shift $\Lambda_{2\pi}$ in the system CO/Ni is larger than in the weak chemisorption system CO/Cu, the image shift $v_{2\pi}$ is, in the present case of strong chemisorption, expected to be more affected by the delocalization than in the system CO/Cu. In this respect the calculated value $v_{2\pi}$(CO/Cu) (Ref. 63) may be safely regarded as an upper bound to the bare image relaxation shifts for normal CO adsorption on metals. Using this as a guideline, and taking into account also the effect of electron-hole pairs of the surface response which shift the resonance maxima upward by about 0.6 eV (cf. discussion and Fig. 1 of Ref. 63), the total dynamic-screening-induced downward shift of the $2\pi^*$ resonance maximum in IPES may take, according to the estimates made for the CO/Cu system, a value smaller than 2.5 eV. Provided the analogy between the properties of the e-h component of the response of the Ni and Cu surface holds, as

it should due to the very general arguments of the Fermi liquid theory, then neglecting a very small variation of $v_{2\pi}$ which might arise from different adsorption geometries, one would have

$$3.1 \text{ eV} > v_{2\pi}^0 > 2.5 \text{ eV} \tag{18}$$

also for the CO/Ni(111) system. This shift is smaller in magnitude than, e.g., the (upward) CO valence-level relaxation shifts $v_{1\pi}^0 = 3.7$ eV and $v_{4\sigma}^0 = 3.6$ eV observed in UPS from the nonbonding orbitals 1π and 4σ of CO adsorbed on polycrystalline Ni (e.g., Ref. 70).

The relation (17a) can now be used to make an order-of-magnitude estimate of the chemical contribution $\Lambda_{2\pi}(\varepsilon_{2\pi}^0 - v_{2\pi}^0)$ to the downward shift of the $2\pi^*$ resonance below ε_V and relative to the position of the affinity level in free CO. According to Eq. (16), $\Lambda_{2\pi}$, as a function of energy, is also relaxation-shift dependent. However, in order to get an order-of-magnitude estimate only, we subtract $v_{2\pi}$ from the total downward shift of the IPES $2\pi^*$ level of CO/Ni(111), which yields

$$\Lambda_{2\pi} > 1.4 \text{ eV} \quad (\text{CO/Ni}) . \tag{19}$$

The nonadiabatic screening of the IPES electron by the substrate electron-hole pairs should occur also for transition-metal substrates, giving rise to extra broadening of the $2\pi^*$-derived resonance above ε_F. The effect should be of the same order of magnitude as found for the system CO/Cu(110),[63] because of the universal properties of soft surface e-h pairs in the Fermi liquids of nearly equal electron density.[38] However, this cannot give rise to large enough broadening of the final IPES spectra, which would explain the total width $\Gamma_{2\pi}$ of the observed $2\pi^*$-derived spectral shapes, because $\Gamma_{2\pi}$ is even larger in the present system than in the case of CO/Cu(110). Hence the observed width of the $2\pi^*$ level in the IPES spectra of CO/Ni(111), together with those of CO/Pd and CO/Pt, may be taken as another piece of direct evidence for the existence of a $2\pi^*$-derived resonance in CO adsorbed on transition metals.

V. $2\pi^*$ RESONANCE MANIFESTATION IN CORE-TO-VALENCE EXCITATION SPECTROSCOPY

Another spectroscopic method which probes unoccupied adsorbate levels by promoting electrons into unoccupied states is x-ray photoabsorption spectroscopy. In this method one measures the absorption rate for photons which induce electronic transitions from occupied localized adsorbate levels (e.g., core states) to unoccupied levels above the Fermi level. The photon absorption rate is proportional to the final density of states of the unoccupied levels. Here the final state is an excited neutral state of the system. The nonradiative relaxation of the system, by which the core hole will eventually be refilled, will involve electron transitions into the core hole (electron deexcitation) accompanied by electron emission from the occupied adsorbate levels including also those broadened into localized bands (resonances) by the hybridization with the substrate valence states. The total electron yield above a certain energy is then proportional to the photoabsorption rate and hence to the density of the unoccupied adsorbate states into which the core electrons have first been excited. Since the deexcitation process provides the energy for electron emission whose yield is measured, this method is sometimes also termed deexcitation electron spectroscopy (DES).[71]

As regards chemisorbed CO, of particular interest are the x-ray-excited core-to-valence transitions, viz., electronic excitations from core O $1s$ and C $1s$ levels into the unoccupied $2\pi^*$-derived states which extend above the substrate Fermi energy. Such measurements have been carried out for the adsorption systems CO/Ni(100),[72,73] CO/Ni(111),[73-76] CO/Pt(111),[77] CO/Cu(100),[78,79] CO/Cu(110),[71] and CO/Ru(001).[75] The common feature of the x-ray absorption spectra obtained in these measurements are several-eV-broad maxima close to the photon energies for which the absorption peaks have also been observed in analogous experiments on free (gas phase) CO, albeit with much sharper linewidths. The characteristic transition frequencies for core- to $2\pi^*$-level excitations in free CO are 287.4 and 534.1 eV for C $1s \rightarrow 2\pi^*$ and O $1s \rightarrow 2\pi^*$, respectively.

In order to get an understanding of the dynamics, energetics, and the manifestation of the $2\pi^*$ resonance features in the core-to-valence excitation spectra, we shall again examine in more detail the systems CO/Cu(110) (Ref. 71) and CO/Ni(111) (Ref. 74) representative of weak and strong chemisorption, respectively, for which the XPS and IPES data have been discussed in Secs. III and IV.

A. Weak chemisorption CO/Cu(110)

In the weak chemisorption system CO/Cu(110) the XPS and IPES experiments indicate the existence of the $2\pi^*$-derived resonance located about 3 eV above ε_F, whose occupation via the backdonation mechanism should be very small. In core-to-valence transition spectra of CO/Cu(110) a maximum was observed at the photon energy $\hbar\omega = 287.5$ eV (Ref. 71) and interpreted as the C $1s \rightarrow 2\pi^*$ excitation. Using the Hamiltonian (1) and the expressions for the chemically induced shift [Eq. (16b)] and the image shifts of the levels involved [cf. Eqs. (2)–(5)], the $1s$ core-to-valence transition energy can be expressed as[46,47,80,81]

$$\varepsilon_{1s\text{-}2\pi} = \varepsilon_{2\pi} - \varepsilon_{1s}^0 - U_{1s,2\pi} + (2v_{1s\text{-}2\pi} - v_{1s} - v_{2\pi}) + \Delta\varepsilon_{\text{scr}} + \Delta\varepsilon_{\text{chem}} , \tag{20}$$

where $\varepsilon_{2\pi}$ incorporates the chemical shift of the $2\pi^*$-derived resonance (now in the presence of the interaction $U_{1s,2\pi}$), and $\Delta\varepsilon_{\text{scr}}$ is the extra-adsorbate screening relaxation shift characteristic of core-to-valence transitions:[38,46,47,50(b)]

$$\Delta\varepsilon_{\text{scr}} \cong v_{2\pi} \left[\frac{\Gamma_{2\pi}^0}{W_{s\text{-}p}} \right]^2 , \tag{21}$$

where $W_{s\text{-}p}$ denotes the width of the substrate valence band which participates in chemisorption. Because

$\Gamma^0_{2\pi} \ll W_{s\text{-}p}$, this shift is going to be very small, of the order of a fraction of an eV.[38,50(b)] The expression (20) will be used discuss various contributions to the energy of core-to-valence transitions. The shape of the peak is characterized by its FWHM, which in the present case is 2.3 eV. The peak exhibits slight asymmetry, with the steeper flank on the low-energy side, and its lower edge is about 1 eV below the peak maximum (cf. Fig. 10).

The peak at 287.5 eV in the adsorption spectrum of CO/Cu(110) is identified as originating from the electron excitation from the C 1*s* core level into the $2\pi^*$-derived resonance of chemisorbed CO. A comparison of the transition energies in the gas and adsorbed phases, which appear to be the same, and the threshold energy of the XPS C 1*s* core spectra of CO adsorbed on Cu(100) [Ref. 9 and Eq. (11)] and on polycrystalline Cu,[11] shows that the maximum in the absorption spectrum occurs on the (110) surface at an energy exceeding the XPS threshold energy by about 1 eV (cf. Fig. 10). In other words, the lower edge of the absorption peak coincides with the XPS core threshold energy, and therefore the $2\pi^*$ *resonance edge* as measured by this spectroscopy is determined by the core-level threshold. Recalling that due to the Pauli exclusion principle the *threshold energy of core-to-valence excitations* $\hbar\omega_{1s\to 2\pi}$ [not to be confused with Eq. (20)] is given by the difference between the energies of the Fermi level and the uppermost state in the core spectrum, these experiments demonstrate that core-to-valence transitions take place between the threshold (*fully relaxed* core-level energy) and the empty states in the $2\pi^*$ resonance *above* the lower resonance edge coinciding with ε_F, viz. that there exists a *unified* threshold for XPS and core-to-valence transitions:

$$|\tilde{\varepsilon}_{1s}| = \hbar\omega^{\text{thrs}}_{1s\text{-}2\pi} = \varepsilon_T \ . \tag{22}$$

The theory of core-to-valence transitions based on the time-dependent treatment of the Hamiltonian of the system [Eq. (1)] (Ref. 47) fully confirms this identification as it predicts the *same* chemically induced relaxation shift [Eq. (3)] for both XPS and absorption spectroscopy [cf. Eq. (6) and (20)]. This enables us to define a unified threshold energy ε_T in chemisorption systems with resonances around ε_F, which in XPS manifests itself as the energy of the relaxed (threshold) core-level peak (relative to ε_F) and in core-to-valence spectroscopy as the minimum energy required to bring an electron from the (upward) relaxed core level to the first unoccupied state in the resonance which lies at ε_F.

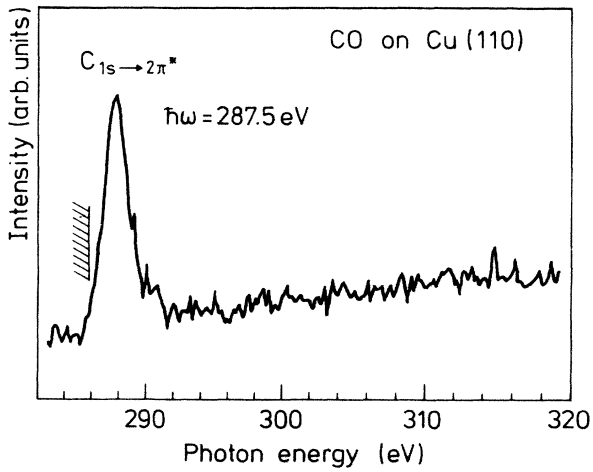

FIG. 10. C $1s\to 2\pi^*$ absorption spectrum for CO/Cu(110) at 100 K (Ref. 79). The hatched edge denotes the XPS C 1*s* threshold.

The comparison of the spectra of the unoccupied part of the $2\pi^*$ resonances in IPES and absorption spectroscopy reveals a difference in both their position and width. In IPES the resonance maximum is at 3.4 ± 0.3 eV above ε_F (at the maximum obtainable coverage),[61] or 0.9 ± 0.3 eV below ε_F. In absorption spectroscopy it is at 1 eV above ε_F as already mentioned above. This implies that the screened electron-hole interaction [Eqs. (1) and (5)] is given by

$$\tilde{U}_{\text{C }1s\text{-}2\pi} = 2.4 \text{ eV} - \Delta\varepsilon_{\text{chem}} \ . \tag{23}$$

Now, $\Delta\varepsilon_{\text{chem}}$ can be estimated by taking the difference of $\tilde{\varepsilon}_{1s}$ [Eq. (6)] in the physisorbed and chemisorbed phases. This yields $\Delta\varepsilon_{\text{chem}} \approx 0.2$ eV for CO/Cu(111), which means a strong reduction of $U_{1s,2\pi}$ from the gas-phase value of about 10 eV,[66] due to the screening by the substrate electrons. From this, and using Eq. (5), we infer that the $2\pi^*$ electron–C 1*s* core-hole image interaction is

$$v_{\text{C }1s\text{-}2\pi} \approx 3.4 \text{ eV} \ , \tag{24}$$

which should also be the order of magnitude of the image relaxation shifts v_{1s} and $v^0_{2\pi}$ in the same system. This also correlates well with the calculated upper bound of the downward image shift of the $2\pi^*$ level for CO adsorption on Cu(110) given by Eq. (14).

The C 1*s*-level relaxation shift can be estimated only roughly from the spectra of CO condensed on noble metals although some caution is needed in making the analogy between the magnitudes of the shifts pertinent to two different adsorption geometries (normal on Cu and flat on Ag, Au, and Al (cf. Sec. III and Table I in Ref. 47). On the other hand, the difference in the electronic structure of the substrate is believed not to affect much the nonbonding image relaxation shifts because the latter derive from universal sum rules on the surface electronic excitations.[38,50,82] This is experimentally supported by photoemission spectra of physisorbed rare gases, e.g., Xe.[83] Thus, subtracting the energies of the C 1*s* levels of free and condensed CO one obtains[47]

$$v_{\text{C }1s} \simeq 4 \text{ eV} \ . \tag{25}$$

With all due caution in making such estimates, the ordering of the magnitudes of the screening shifts then reads

$$v_{\text{C }1s} > v_{\text{C }1s\text{-}2\pi} > v^0_{2\pi} \tag{26}$$

and agrees well with the notion that the image shifts should be larger the more localized the charge in the orbital in question is and the closer its center of gravity is located towards the substrate image plane.[84] For normal CO adsorption the localized C 1*s* orbital is closer to the substrate than the center of gravity of the $2\pi^*$ electron

density (|wave function|^2) residing on CO and this may be used as a qualitative argument to estimate that $v_{C\,1s} > v^0_{2\pi}$. According to the same argument the repulsion between the diffuse electron density of the $2\pi^*$ electron and much more localized image charge density of the $1s$ hole should produce $v_{1s\text{-}2\pi}$ lying between the other two shifts, as indeed indicated in Eq. (26).

The width (FWHM) of the resonance in C $1s \rightarrow 2\pi^*$ transitions in CO/Cu(110) is 2.3 eV,[71] which is 0.7 eV smaller than the $2\pi^*$ resonance width in IPES.[61] The extra width in IPES may be attributed to several different initial-state effects (e.g., coverage-dependent resonance dispersion) and final-state effects (nonadiabatic screening of the IPES electron, cf. Sec. IV). In core-to-valence transitions the adsorbate remains neutral and the effect of the substrate dynamic screening on the spectral shape should be negligible for the same reason, which explains the reduction of the image shift $\Delta\varepsilon_{scr}$ [Eq. (21)] in absorption spectroscopy. The apparent asymmetry of the resonance peak in absorption spectra may occur due to the cutoff in the core-to-valence excitation spectrum at the threshold energy ε_T [Eq. (20)]. Here ε_F may lie within the resonance because the whole peak is shifted down by $\tilde{U}_{C\,1s\text{-}2\pi}$ with respect to the IPES case, and hence much closer to ε_F. This feature will be discussed in more detail below in connection with strong CO adsorption on Ni. Finally, the bare resonance width $\Gamma^0_{2\pi}$ depends, in general, on the position of the resonance center with respect to the substrate valence-band edges and the spatial extension of the $2\pi^*$ orbital in the final state. As this position differs in IPES and absorption spectra by $\tilde{U}_{1s\text{-}2\pi}$, the variation of the resonance width due to this effect, and the fact that $2\pi^*$ is also more contracted in the presence of the core hole[7(b)] which reduces the resonance tunneling width, can contribute to the observed differences in the resonance bandwidth.

On studying the partial photoelectric yield in core-to-valence transitions and on comparing it with the corresponding Auger and photoemission spectra, one can also learn a lot about the physics of relaxation and deexcitation processes subsequent to the core-hole creation in these spectroscopies. The comparison of the CO/Cu(110) Auger spectra following photoemission (excitation energy $\hbar\omega = 3111$ eV) and core-to-valence excitations (excitation energy $\hbar\omega = 287.5$ eV),[71] shows an agreement between the binding energies of the 4σ and $(1\pi + 5\sigma)$ peaks in the spectra only if both are referred to the energy of the C $1s$ threshold $\tilde{\varepsilon}_{C\,1s} = 286.5$ eV as the initial energy available for the Auger deexcitation. This agreement is lacking if the C $1s \rightarrow 2\pi^*$ resonant excitation energy $\hbar\omega_{C\,1s\text{-}2\pi} = 287.5$ eV is taken as the reference energy (see Fig. 11). The UPS data ($\hbar\omega = 35$ eV), on the other hand, revealed full agreement in the binding-energy assignment between the UPS and Auger spectra recorded after photoionization with $\hbar\omega = 311$ eV.[71]

The energetics of the deexcitation process following the photoionization and core-to-valence transition, based on the discussion of the preceding paragraph and on the dynamics contained in the Hamiltonian (1), is sketched in Figs. 12(a) and 12(b). The deexcitation process after photoionization [$\hbar\omega = 311$ eV in Fig. 12(a)] involves an electronic transition which fills up the core hole in the fully relaxed, final state at threshold energy $\tilde{\varepsilon}_{C\,1s}$. The electron is suppled either from a state at the Fermi level of the substrate valence band or, more likely, due to a larger transition amplitude, from a state at the Fermi level in the partly filled $2\pi^*$ *resonance in the final relaxed state.* The available Auger energy from such a transition is then given by the core-level threshold energy ε_T [Eq. (22)]. Here it is important to point out that in discussing the deexcitation energy both levels involved (viz. C $1s$ and $2\pi^*$) should be considered in the relaxed state because the relaxation and the threshold energy of the core hole are determined by the relaxation and screening processes within the resonance which is first pulled down by $\tilde{U}_{C\,1s\text{-}2\pi}$ and then partially filled by the charge transfer. All these processes are much faster than the core-hole decay, as confirmed experimentally by the availability of a unique Auger excitation energy[71] equal to ε_T.

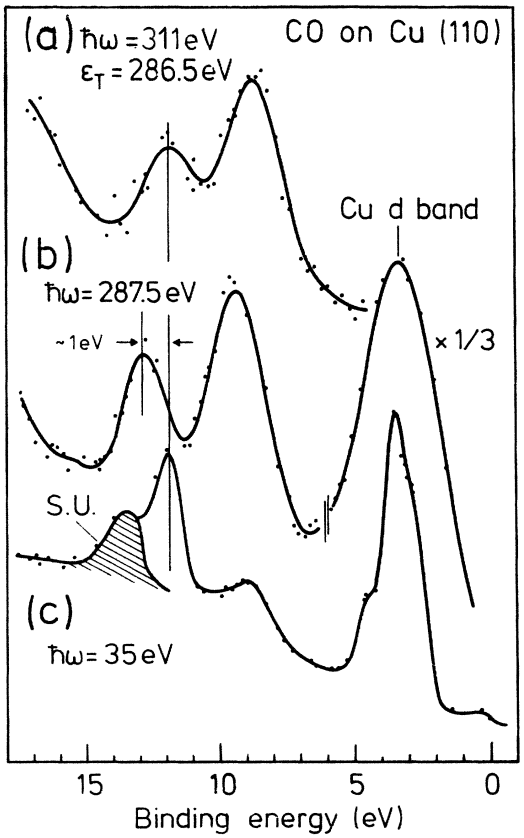

FIG. 11. Comparison of the binding energies for the single-hole valence portions of (a) the Auger spectrum corresponding to the excitation energy $\hbar\omega = 311$ eV, (b) the deexcitation spectrum following C $1s \rightarrow 2\pi^*$ excitation, and (c) the direct photoemission. The Cu $3d$ bands seen in (b) are excited by direct photoemission, not by the core-hole decay process (from Ref. 79). The shaded peak (S.U.) in curve (c) is the 4σ shake-up. Note the shift of 1 eV between spectra (a) and (b), which is discussed in the text.

In the deexcitation process following the core-to-valence transition [Fig. 12(b)] the excited electron in the $2\pi^*$ resonance will provide a local screening of the core

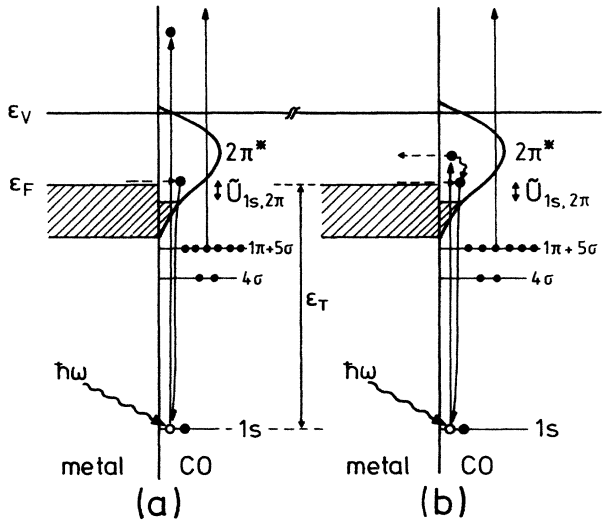

FIG. 12. Schematic energy-level diagram for core-hole deexcitation following (a) photoionization in XPS and (b) $1s \rightarrow 2\pi^*$ transition. In (a) a core electron is ejected above ε_V and core screening proceeds via electron transfer from the substrate Fermi level into the resonance (dashed arrow pointing right). In (b) the core electron excited into the resonance either tunnels out (dashed arrow pointing left) or makes an intraresonance transition to ε_F (wiggly arrow). In both cases the Auger energy released in the core deexcitation equals ε_T and may lead to the emission of an Auger electron (e.g., out of the $1\pi+5\sigma$ and 4σ levels).

hole as long as it remains in one of the resonance states. However, as the resonance states are lifetime broadened, and as such a configuration with an excited electron about 1 eV above ε_F in the (downward shifted) resonance will be highly unstable, so relaxation processes, similar to those following the photoionization in XPS, will take place. There are two possible decay channels through which the excited $2\pi^*$ electron can be brought to ε_F and thereby the whole system to a fully relaxed state which is identical to the core-hole relaxed state of XPS. First, the electron may tunnel out of the resonance with a decay rate which is given by $\Gamma^0_{2\pi}(\tilde{\varepsilon}_{2\pi})$. Once in the substrate valence band, the electron may eventually thermalize, i.e., make a transition to ε_F. *Simultaneously,* an electron from the Fermi level from the substrate may tunnel into the resonance states pulled down below ε_F by $\tilde{U}_{1s\text{-}2\pi}$ and this process proceeds at the time rate $\Gamma^0_{2\pi}(\varepsilon_F)$. These events are indicated by dashed horizontal arrows in Fig. 12(b). Both processes are very fast and bring the system into the fully relaxed state with screened core hole. The hole may then decay through the Auger deexcitation process whose deexcitation energy is then given by the threshold energy ε_T, as in photoionization.

The second possibility is that the excited $2\pi^*$ electron makes a transition within the resonance, from the state of energy $\tilde{\varepsilon}_{2\pi}$ to a state at ε_F [Fig. 12(b), wiggly arrow]. Such a direct intraresonance thermalization process will be possible either if one or more electrons in the system, which are coupled by the interactions with the resonance charge density fluctuations, are excited (radiationless decay), or if other degrees of freedom which constitute the heat bath of the system will absorb directly the energy released in the intraresonance transition. The probability of such intraresonance electronic transition is given by the corresponding oscillator strength which, due to the energy continuum within the resonance, is a function of the transition energy. It has been shown[34,35,82] that the intraresonance oscillator strength per unit energy interval $f_{2\pi}(\varepsilon)$ is given by the self-convolution of the resonance density of states $\rho^0_{2\pi}(\varepsilon)$. For resonances located close to ε_F this convolution has a maximum for transition energies around $\Gamma^0_{2\pi}(\varepsilon_{2\pi})$ [cf. Fig. 13 in Ref. 38 and Fig. 5(b) in Ref. 82(b)]. Hence, the intraresonance channel of thermalization of the excited $2\pi^*$ electron is also a possible process whose probability is proportional to the density of the electron final states $\rho_{2\pi}(\varepsilon_F)$. This relaxation process is denoted by a wiggly arrow in Fig. 12(b) and leads to the *same* final screened core-hole state as in the case of relaxation by resonance tunneling, and both lead to the *same* final screened state as in the photoionization process depicted in Fig. 12(a). Of course, identical implications on the subsequent Auger decay processes, their spectra, and energetics, hold also in this case. In particular, the relaxed state after the core-to-valence transition will be identical to that subsequent to XPS, giving rise to the same Auger decay processes. This enables us now to interpret the Auger spectra following the C $1s$ core$\rightarrow 2\pi^*$ valence-level electronic excitations in CO/Cu(110) reported in Ref. 71 and reproduced in Fig. 11. Although the excitation energy $\hbar\omega_{1s\rightarrow 2\pi}$ in this case was 287.5 eV, i.e., ε_T+1 eV, the peak energies of the observed Auger spectrum were found to correspond to the *effective* excitation energy equal to ε_T. Thus the excess energy of 1 eV noticed by the authors of Ref. 71 is precisely that energy which the electron excited into the resonance releases to the system during the thermalization to the Fermi level. This interpretation is also strongly supported by the equivalent shapes of the C(KLL) and O(KLL) Auger spectra of CO/Ni(111)[79] for various core-hole excitation energies.

To summarize the present discussion, we reiterate that these findings demonstrate the relevance of the unified threshold energy ε_T [Eq. (22)] discussed above and the importance of the resonance-induced relaxation process subsequent to the core-hole creation in both XPS and absorption spectroscopy. Moreover, the $2\pi^*$ resonance model provides also an explanation for the similarity of the photoionization- and photoabsorption-induced Auger valence spectra in CO/Cu, and removes the query about the energy imbalance pointed out by Chen *et al.*[71] in the assignment of the characteristic Auger valence 4σ and $(1\pi+5\sigma)$ peaks of the CO/Cu (110) system.

B. Strong chemisorption: CO/Ni(111)

To discuss the $2\pi^*$ resonance features in core-to-valence spectra of strong chemisorption systems we choose CO/Ni(111) for which the UPS,[17] XPS,[17] and IPES (Ref. 66) data are also available for comparison. The C $1s\rightarrow 2\pi^*$ and O $1s\rightarrow 2\pi^*$ absorption spectra are shown in Fig. 13,[74] together with the corresponding XPS

core 1s spectra,[17,85] shown on the same energy scale, with the binding energy increasing to the right in order to facilitate the comparison of the threshold energies. The maxima of the spectra define the transition energies [Eq. (20)]

$$\varepsilon_{O\ 1s-2\pi}=532.4\ \text{eV}\ ,\qquad \varepsilon_{C\ 1s-2\pi}=287\ \text{eV}\ , \tag{27}$$

which differ from the corresponding gas-phase values 531.4 eV and 287.3 eV, respectively (see Table I in Ref. 47), due to the screening and chemisorption effects. The FWHM of the peaks are

$$\Gamma_{2\pi}\Big|_{C\ 1s\rightarrow 2\pi}=2.2\ \text{eV}\ ,\qquad \Gamma_{2\pi}\Big|_{O\ 1s\rightarrow 2\pi}=3.5\ \text{eV}\ . \tag{28}$$

Both peaks can clearly be identified with the $2\pi^*$ final-state resonance structure because the resolution broadening in these measurements was lower by an order of magnitude (0.17 eV for the C 1s level[86]) than the corresponding peak width. The alignment of the XPS core threshold maxima with the resonance edges at the lower-energy side demonstrates the existence of unified threshold energies ε_T for both types of spectra and for both core levels:

$$|\tilde{\varepsilon}_{C\ 1s}|=\hbar\omega^{\text{thrs}}_{C\ 1s-2\pi}=285.3\ \text{eV}=\varepsilon_T(C\ 1s)\ ,\qquad |\tilde{\varepsilon}_{O\ 1s}|=\hbar\omega^{\text{thrs}}_{O\ 1s-2\pi}=530.8\ \text{eV}=\varepsilon_T(O\ 1s)\ , \tag{29}$$

$\tilde{\varepsilon}_{1s}$ being measured relative to ε_F. The smaller downward shift of the peak maximum and its smaller width in the case of C1$s\rightarrow 2\pi^*$ transitions is evident and can easily be explained by the chemical properties of the resonance in the final state.[7(b)] Namely, in the O 1$s\rightarrow 2\pi^*$ transitions the density of the $2\pi^*$ excited electron is larger at the carbon end of the adsorbed CO molecule (i.e., closer to the substrate), while in the C 1$s\rightarrow 2\pi^*$ transition the situation is just the reverse. Hence, it is expected that the hybridization matrix element V_{km} in Eq. (1) would be larger in the former case, leading to a larger final-state resonance width $\Gamma^0_{2\pi}$ for the O 1s core excitation, and possibly to a correspondingly larger chemical contribution $\Lambda_{2\pi}$ to the energy shift of the $2\pi^*$ resonance. The chemically induced relaxation shifts $\Delta\varepsilon_{\text{chem}}$ can be estimated by taking the difference of XPS core-level energies $\tilde{\varepsilon}_{1s}$ [Eq. (6)], or the differences of NEXAFS transition energies $\varepsilon_{1s-2\pi}$ [Eq. (20)] for chemisorbed, physisorbed, and gaseous CO.[47] Since the differences obtained from the NEXAFS data contain also the change of the resonance chemical shifts $\Delta\Lambda_{2\pi}$ arising as the consequence of the change of the hybridization strength due to the switching on of the interaction $\tilde{U}_{1s-2\pi}$ [Eq. (5)], the values of $\Delta\varepsilon_{\text{chem}}$ obtained from the XPS data should be considered as more reliable. Thus one gets [cf. also Table I and Eq. (12) in Ref. 47]:

$$\Delta\varepsilon_{\text{chem}}(O\ 1s)=1.55\ \text{eV}\ ,\qquad \Delta\varepsilon_{\text{chem}}(C\ 1s)=0.9\ \text{eV}\ , \tag{30}$$

for the holes on the O 1s and C 1s orbitals of CO/Ni(11), respectively. The values estimated from the NEXAFS spectra differ from these only slightly.[47] The magnitudes of $\Delta\varepsilon_{\text{chem}}$ in Eq. (30) show clearly that the chemical effects should be larger in the O 1s hole excited configuration. This conclusion is reinforced by the calculation of the potential energy curves of the O 1$s\rightarrow 2\pi^*$ and C 1$s\rightarrow 2\pi^*$ excited Cu_5CO clusters which give larger metal-CO bonding energy, and hence larger chemical interaction for the O 1$s\rightarrow 2\pi^*$ excited state of the cluster.[7] It is illustrative to compare the widths and the shapes of the resonances showing up in core-to-valence transitions with the ones revealed by IPES (cf. Ref. 66 and Sec. IV). Besides the shift of the resonance maximum which is due to the different final state interaction described by $\tilde{U}_{1s-2\pi}$ in Eq. (1), the smaller widths of the resonances in the absorption spectra are noticeable.

The IPES $2\pi^*$ resonance FWHM in CO/Ni(111) exceeds 3 eV,[66] whereas the widths of the absorption spectra given by Eq. (27) are somewhat smaller. The IPES resonance shape in CO/Ni(111) exhibits some asymmetry which can be interpreted on the same grounds as for the CO/Cu(110) system (Sec. IV). Although this asymmetry can give rise to additional broadening of the $2\pi^*$ IPES spectra of CO/Ni(111) over the bare chemically induced FWHM $\Gamma^0_{2\pi}$, the smaller peak widths in core-to-valence spectra may in part be due to the occupation of a part of the resonance extending below the threshold (i.e., below ε_F). This occupation makes that part of the resonance inaccessible to core electrons and hence invisible in the absorption spectroscopy. A bare inspection of Fig. 13 and the positions of the thresholds shows that the occupied parts of the resonances (in the relaxed state) may extend below ε_F. Incidentally, if the $2\pi^*$ resonance in the O 1$s\rightarrow 2\pi^*$ spectrum were symmetric around the peak maximum, its FWHM would be about 4 eV, close to that in IPES. However, in C 1$s\rightarrow 2\pi^*$ transitions the resonance width is too small to allow for such a speculation. The main reason, however, for the reduction of the width in this case is the weaker CO-metal bonding in the C 1$s\rightarrow 2\pi^*$ excited-electron configuration than in the ground state of the system.[7]

Another peculiarity of the CO/Ni(111) core-to-valence spectra noticeable in Fig. 13 is their shape at the threshold. In the one-electron picture the spectral shape of the transitions should reflect the density of one-electron states in the unoccupied part of the resonance. In this picture a rather sharp cutoff should occur in the spectrum at the threshold (i.e., ε_F, see Fig. 14). This cutoff can be smeared-out by resolution broadening, core hole lifetime effects, or excitation of the vibrational degrees of freedom in the system. The resolution in the experiments which yielded Fig. 13 were very high[86] and for other dynamic effects one may assume the adiabatic regime. However, the shape of the resonance edge at the threshold looks in both cases more like a rise from zero (after background subtraction) to some finite value than a smeared-out cutoff. Also, any smearing-out of the cutoff due to resolution etc., would appear more or less even around the threshold, whereas the spectra of Fig. 13 drop rather sharply from the resonance maximum down to a

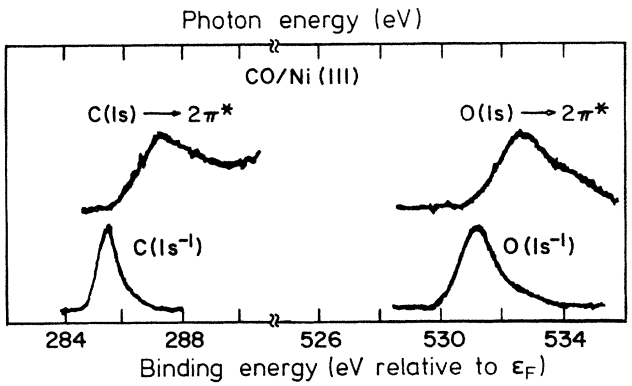

FIG 13. Comparison of XPS $1s$ and absorption $1s \rightarrow 2\pi^*$ spectra on the same energy scale for carbon and oxygen of CO adsorbed on Ni(111), showing the relation between the screened ionic photoemission states and the neutral electronic excitation states. (From Ref. 74.)

minimum at ε_T. This behavior can be explained by an interplay of the singular scattering of the excited $2\pi^*$ electron off the $1s$ core hole with the singular shakeup screening of the core hole by the electrons residing in the resonance in the initial state (analogous to those in XPS, cf. Sec. III C).[36,38,47] The dynamics of both processes is typical of a many-body response to a localized transient perturbation $\tilde{U}_{1s\text{-}2\pi}$.[53] In the present case it may lead to a power-lay quenching of the absorption spectrum at the threshold due to the singular scattering of electrons by the core hole. The discussion of this effect has been given in more detail in Ref. 47. and here we outline it only briefly.

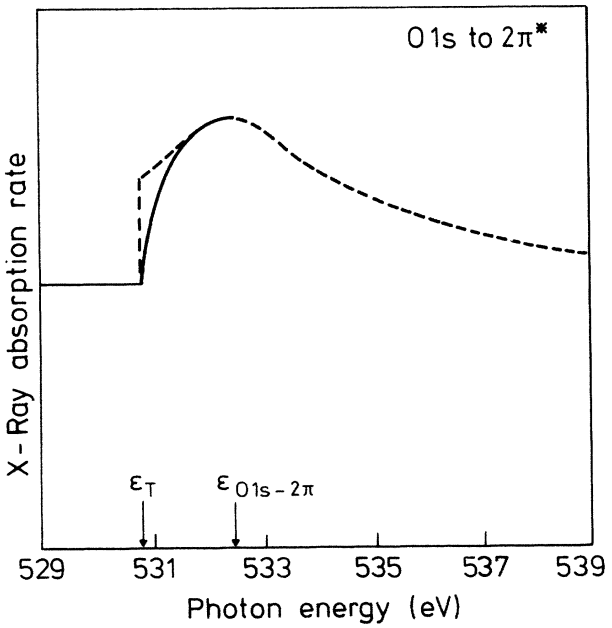

FIG. 14. Optical absorption rate [Eq. (30)] for the O $1s \rightarrow 2\pi^*$ core-to-valence electronic transition. Dashed line, absorption rate in the one-electron picture; solid line, threshold softening of the spectrum due to the shake-up relaxation processes for $\alpha < 0$. (From Ref. 47.)

The scattering of an electron in the (m,σ) channel of the resonance, caused by the core-hole potential $\tilde{U}_{1s\text{-}2\pi}$, is described by the phase shift $\delta_{m\sigma}(\varepsilon)$ [Eq. (4)] which may reach a maximum value of $\pi/2$ when the denominator on the right-hand side of Eq. (4) vanishes (case of resonant scattering). The absorption spectrum in the threshold region is affected by the effect of singular scattering and takes the form

$$\lim_{\varepsilon \rightarrow \varepsilon_T} S_{1s\text{-}2\pi}(\varepsilon) = \sum_{m,\sigma} \frac{\rho^0_{m\sigma}(\varepsilon_F)}{[\rho^0_{m\sigma}(\varepsilon_F)(\varepsilon - \varepsilon_F)]^{\alpha}} \Theta(\varepsilon - \varepsilon_T) , \tag{31}$$

where α is again given by Eq. (9). However, since in core-to-valence transitions one electron is supplied by the core hole in the transition channel (l,ν), the numbers $n_{m\sigma}$ are here given by [cf. Eq. (10)]

$$n_m = \begin{cases} \delta_{m\sigma}(\varepsilon_F)/\pi - 1, & (m,\sigma) = (l,\nu) \\ \delta_{m\sigma}(\varepsilon_F)/\pi, & \text{all other channel} . \end{cases} \tag{32}$$

The absorption rate [Eq. (31)] may therefore be either singular ($\alpha > 0$) or zero ($\alpha < 0$), depending on the magnitude of the sum of the squares of the extra screening electrons in each channel.

The phase shifts $\delta_{m\sigma}(\varepsilon_F)$ need not be equal for all four resonance channels derived from the fourfold-degenerate (including spin) $2\pi^*$ level. In the case of strong chemisorption when $\Gamma^0_{2\pi}(\varepsilon_F)$ may be large enough, the absolute values of the phase shifts may approach the resonant values so as to give rise to $\alpha < 0$. According to Eq. (31) this would lead to a power-law quenching of the absorption spectrum $S_{1s\text{-}2\pi}(\varepsilon)$ at the threshold, in the fashion shown in Fig. 14, and similar to the behavior found experimentally. The power-law quenching of the absorption spectrum depends critically on two conditions: (a) the existence of the $2\pi^*$ resonance in the initial and final state, and (b) the partial resonance occupation in the initial state [i.e., $\Gamma^0_{2\pi}(\varepsilon_F) \neq 0$]. It is a typical many-body feature which may therefore serve as additional evidence for the hybridization-induced broadening of the $2\pi^*$ level into a relatively broad resonance overlapping ε_F. Because of the quenching at the threshold and due to the proximity of ε_T to the resonance maximum, it would not be justified to identify the first moment of the absorption spectrum with the energy of the resonance, but rather its maximum. The latter is, according to the above discussion, much less affected by the transient perturbations and dynamic screening effects than the first moment of the spectrum.

VI. CONCLUSIONS

The failure of the traditional MO model to interpret certain aspects of the electronic spectra of CO adsorbed on Cu and transition metals, as investigated by electron spectroscopies (UPS, SPIES, XPS), inverse photoemission and x-ray absorption spectroscopy (NEXAFS), has led us to analyze the spectral data of adsorbed CO within the $2\pi^*$ resonance model of CO chemisorption. The analyses in Secs. III–V show that the measured spectra exhibit,

besides the method-specific features, also certain common characteristics which may be regarded as manifestations of or originating from the chemical and physical properties of a fractionally occupied $2\pi^*$-derived adsorbate resonance. As demonstrated in our discussions, these features are not only restricted to the spectra of CO $2\pi^*$-derived levels themselves, but also show up in the spectra of the adsorbate core levels and core-to-valence transitions. Moreover, the dynamical relaxation processes associated with the partially occupied resonances are shown to give rise to unified core-level shifts, threshold energies, and spectral broadening effects whose observed features are otherwise not possible to explain within the MO types of models of CO chemisorption. The ability of the $2\pi^*$ resonance model to provide a *unified* qualitative and even semiquantitative interpretation of the adsorbate spectral properties may be taken as a strong support for the actual existence of the $2\pi^*$-derived electronic resonances in CO/Cu and CO/transition metal adsorption complexes.

ACKNOWLEDGMENTS

The cooperation between the institutions of the first two authors (B.G. and K. W.) was partly supported by Zavod za medjunarodnu tehničku suradnju (YU-ZAMS), Zagreb and Internationales Büro der KFA, Jülich. The communication of the experimental data from Y. Jugnet and F. J. Himpsel is gratefully acknowledged.

[1]T.-C. Chiang, G. Kaindl, and D. E. Eastman, Solid State Commun. **36**, 25 (1980).

[2](a) D. Schmeisser, F. Greuter, W. Plummer, and H.-J. Freund, Phys. Rev. Lett. **54**, 2095 (1985); (b) S. Krause, C. Mariani, K. C. Prince, and K. Horn, Surf. Sci. **138**, 305 (1984); (c) Ph. Avouris and J. E. Demuth, Surf. Sci. **158**, 21 (1985).

[3]F. J. Himpsel, R. A. Pollack, and E. E. Koch (private communication).

[4]The fact that *all* molecular levels shift by the *same* amount upon adsorption is, by itself, the best definition for the existence of pure physisorption interaction; see, e.g., K. Jacobi and H. H. Rotermund, Surf. Sci. **116**, 435 (1982).

[5]G. Blyholder, J. Chem. Phys. **68**, 2772 (1964).

[6]G. Doyen and G. Ertl, Surf. Sci. **43**, 197 (1974).

[7](a) P. S. Bagus, C. J. Nelin, and C. W. Bauschlicher, J. Vac. Sci. Technol. A **2**, 905 (1984); (b) Ph. Avouris, P. S. Bagus, and A. R. Rossi, J. Vac. Sci. Technol. B **3**, 1484 (1985), and references therein.

[8]H. Ibach and D. L. Mills, *Electron Energy Loss Spectroscopy* (Academic, New York, 1982), and references therein.

[9]C. R. Brundle and K. Wandelt, in *Proceedings of the Seventh International Vacuum Congress and the Third International Conference on Solid Surfaces (Vienna, 1977)*, edited by R. Dobrozemsky, F. Rüdenauer, F. P. Viehböck, and A. Breth, (unpublished), p. 1171.

[10]C. L. Allyn, T. Gustafsson, and E. W. Plummer, Solid State Commun. **24**, 531 (1977).

[11]P. R. Norton, R. L. Tapping, and J. W. Goodale, Surf. Sci. **72**, 33 (1978).

[12]S. A. Lindgren, J. Paul, and L. Wallden, Chem. Phys. Lett. **84**, 487 (1981).

[13]C. F. McConville, C. Somerton, and D. P. Woodruff, Surf. Sci. **139**, 75 (1984).

[14]Y. Jugnet and Tran Minh Duc, Chem. Phys. Lett. **58**, 243 (1978).

[15]P. R. Norton, R. L. Tapping, and J. W. Goodale, Chem. Phys. Lett. **41**, 247 (1976).

[16]C. R. Brundle, P. S. Bagus, D. Menzel, and K. Hermann, Phys. Rev. B **24**, 7041 (1981).

[17]Y. Jugnet, Ph.D. thesis, Université Claude Bernard, Lyon, 1981.

[18]G. Broden, T. N. Rhodin, C. Brucker, R. Benbow, and Z. Hurych, Surf. Sci. **59**, 593 (1976).

[19]R. Miranda, K. Wandelt, D. Rieger, and R. D. Schnell, Surf. Sci. **139**, 430 (1984).

[20]F. Greuter, D. Heskett, E. W. Plummer, and H.-J. Freund, Phys. Rev. B **27**, 7117 (1983).

[21](a) P. G. Page and P. M. Williams, in Faraday Discuss Chem. Soc. **58**, (1975); (b) P. M. Williams, P. Butcher, J. Wood and K. Jacobi, Phys. Rev. B **14**, 3215 (1976); (c) R. J. Smith, J. Anderson and G. J. Lapeyre, Phys. Rev. Lett. **37**, 1081 (1976); in *Proceedings of the International Symposium on Photoemission, Nordwijk, 1976*, edited by R. F. Willis, B. Feuerbacher, B. Fitton and C. Backx (European Space Agency, Paris, 1976), p. 249.

[22](a) R. A. Shigeishi and D. A. King, Surf. Sci. **58**, 484 (1976); (b) H. Conrad, G. Ertl, H. Knözinger, J. Küppers, and E. E. Latta, Chem. Phys. Lett. **42**, 115 (1976); (c) J. Küppers, H. Conrad, G. Ertl, and E. E. Latta, Jpn. J. Appl. Phys. Suppl. 2, Pt. 2, **225**, (1974); Surf. Sci. **57**, 475 (1976); (d) G. Ertl, J. Vac. Sci. Technol. **14**, 435 (1977); (e) T. Gustafsson, E. W. Plummer, D. E. Eastman, and J. L. Freeouf, Solid State Commun. **17**, 39 (1975); (f) T. Gustafsson and E. W. Plummer in *Proceedings of the International Symposium on Photoemission, Nordwijk, 1976*, Ref. 21(c), p. 255; (g) E. W. Plummer, in *Proceedings of the Seventh International Vacuum Congress and the Third International Conference on Solid Surfaces (Vienna, 1977)*, Ref. 9, p. 647.

[23]J. C. Fuggle, M. Steinkilberg, and D. Menzel, Chem. Phys. **11**, 307 (1975).

[24]Ph. Avouris, P. S. Bagus, and C. J. Nelin, J. Electron. Spectrosc. **38**, 269 (1986).

[25](a) D. Rieger, Ph. D. thesis, University of München, 1985; (b) D. Rieger, R. D. Schnell, and W. Steinmann, Surf. Sci. **143**, 157 (1984), and references therein.

[26]C. L. Allyn, T. Gustafsson, and E. W. Plummer, Chem. Phys. Lett. **47**, 127 (1977).

[27]M. A. van Hove, W. H. Weinberg and C.-M. Chan, *Low Energy Electron Diffraction, Experiment, Theory and Surface Structure Determination*, Vol. 6 of *Springer Series in Surface Sciences* (Springer, Heidelberg, 1986).

[28](a) W. Riedl and D. Menzel, Surf. Sci. **163**, 39 (1985) (b) W. Riedl and D. Menzel, *Proceedings of the DIET II Conference, October 1984*, Vol. 4 of *Springer Series in Surface Sciences*, (Springer, Heidelberg, 1985), p. 136. (c) J. T. Yates, Jr., C. Klauber, M. D. Alvey, H. M. Metiu, J. Lee, R. Martin, J. Arias, and C. Hanrahan, *ibid.*, p. 123; (d) M. D. Alvey, M. J. Dresser, and J. T. Yates, Jr., Surf. Sci. **165**, 447 (1986); (e) H.

Kuhlenbeck, M. Neumann, and H.-J. Freund, Surf. Sci. **173**, 194 (1986).
[29](a) Ph. Avouris, Phys. Scr. **35**, 47 (1987); (b) Shin-ichi Ishi, Yu-ichi Ohno, and B. Viswanathan, Surf. Sci. **161**, 349 (1985).
[30](a) D. M. Newns, Phys. Rev. **178**, 1123 (1969); (b) J. P. Muscat and D. M. Newns, Prog. Surf. Sci. **9**, 1 (1978).
[31]N. D. Lang and A. R. Williams, Phys. Rev. Lett. **34**, 531 (1975); **37**, 212 (1976).
[32](a) B. I. Lundquist, O. Gunnarsson, and H. Hjelmberg, Surf. Sci. **89**, 196 (1979), and references therein; (b) H. Hjelmberg, Phys. Scr. **18**, 481 (1978).
[33]J. P. Muscat, Prog. Surf. Sci. **18**, 59 (1985), and references therein.
[34]B. Gumhalter and K. Wandelt, Phys. Rev. Lett. **57**, 2318 (1986).
[35]K. Wandelt and B. Gumhalter, Surf. Sci. **169**, 138 (1986).
[36]B. Gumhalter, J. Phys. C **10**, L219 (1977).
[37]B. Gumhalter, Phys. Rev. B **19**, 2018 (1979).
[38]B. Gumhalter, Prog. Surf. Sci. **15**, 1 (1984).
[39]H. Conrad, G. Ertl, J. Küppers, S. W. Wang, K. Gerard, and H. Haberland, Phys. Rev. Lett. **42** 1082 (1979).
[40](a) H. Conrad, G. Ertl, J. Küppers, W. Sesselmann, and H. Haberland, Surf. Sci. **121**, 161 (1981); (b) H. Conrad, Habilitation thesis, University of Müchen, 1983; (c) W. Sesselmann, Ph.D. thesis, University of München, 1983.
[41]A. Niehaus, Adv. Chem. Phys. **45**, 399 (1981).
[42]W. Sesselmann, B. Woratschek, G. Ertl, J. Küppers, and H. Haberland, Surf. Sci. **146**, 17 (1984).
[43]F. Bozso, J. T. Yates, Jr., J. Arias, H. Metiu, and R. M. Martin, J. Chem. Phys. **78**, 4256 (1983).
[44]J. Lee, C. P. Hanrahan, J. Arias, R. M. Martin, and H. Metiu, Phys. Rev. Lett. **51**, 1803 (1983).
[45]The emission observed in the Penning spectra between ε_F and 4 eV could laso be interpreted as metal-adsorbate antibonding level as a consequence of σ^- donor coupling between occupied adsorbate and metal states (Ref. 42).
[46]B. Gumhalter and D. M. Newns, Phys. lett. **57A**, 423 (1976).
[47]B. Gumhalter, Phys. Rev. B **33**, 5245 (1986).
[48]K. Schönhammer and O. Gunnarsson, Solid State Commun. **23**, 691 (1977).
[49](a) J. W. Gadzuk and S. Doniach, Surf. Sci. **77**, 427 (1978); (b) B. N. J. Person and Ph. Avouris, J. Chem. Phys. **79**, 5156 (1983).
[50](a) B. Gumhalter and D. M. Newns, Phys. Lett. **53A**, 137 (1975); (b) B. Gumhalter, J. Phys. (Paris) **38**, 1117 (1977).
[51](a) N. D. Lang and A. R. Williams, Phys. Rev. B **16**, 2408 (1977); (b) for a more extended discussion and references see B. Feuerbacher, B. Fitton, and R. F. Willis, *Photoemission and the Electronic Properties of Surfaces* (Wiley Interscience, New York, 1978).
[52]P. W. Anderson, Phys. Rev. Lett. **18**, 1049 (1967).
[53]P. Nozieres and C. T. De Domincis, Phys. Rev. **178**, 1097 (1969).
[54]J. C. Fuggle, E. Umbach, D. Menzel, K. Wandelt, and C. R. Brundle, Solid State Commun. **27**, 65 (1978).
[55]E. Umbach, Surf. Sci. **117**, 482 (1982).
[56]O. Gunnarsson and K. Schönhammer, Solid State Commun. **26**, 147 (1978).
[57]O. Gunnarsson and K. Schoñhammer, Phys. Rev. Lett. **41**, 1608 (1978).
[58](a) V. Dose, Prog. Surf. Sci. **13**, 225 (1983); (b) Surf. Sci. Rep. **5**, 337 (1985).
[59]Th. Forster, F. J. Himpsel, J. J. Donelon, and A. Marx, Rev. Sci. Instrum. **54**, 68 (1983).
[60]J. B. Pendry, Phys. Rev. Lett. **45**, 1356 (1980).
[61]J. Rogozik, H. Scheidt, V. Dose, K. C. Prince, and A. M. Bradshaw, Surf. Sci. **145**, L481 (1984).
[62]J. Rogozik, V. Dose, K. C. Prince, A. M. Bradshaw, P. S. Bagus, K. Hermann, and Ph. Avouris, Phys. Rev. B **32**, 4296 (1985).
[63]B. Gumhalter, Surf. Sci. **157**, L355 (1985).
[64]P. Nordlander and Ph. Avouris, Surf. Sci. **177**, L1004 (1986).
[65]Ph. Avouris, R. Kawai and D. M. Newns (unpublished).
[66](a) F. J. Himpsel and Th. Fauster, Phys. Rev. Lett. **49**, 1583 (1982); (b) Th. Fauster and F. J. Himpsel, Phys. Rev. B **27**, 1390 (1983).
[67]J. Rogozik, J. Küppers, and V. Dose, Surf. Sci. **148**, L653 (1984).
[68]S. Ferrer, K. H. Frank, and B. Reihl, Surf. Sci. **162**, 264 (1985).
[69]B. Gumhalter, Prog. Surf. Sci. **15**, 1 (1984), see Sec. 5 B.
[70]C. R. Brundle and A. F. Carey, Faraday Discuss. Chem. Soc. **60**, 51 (1975).
[71]C. T. Chen, R. A. DiDio, W. K. Ford, E. W. Plummer, and W. Eberhardt, Phys. Rev. B **32**, 8434 (1985).
[72]J. Stöhr, K. Baberschke, R. Jaeger, R. Treichler, and S. Brennan, Phys. Rev. Lett. **47**, 381 (1981).
[73]R. F. Davis, S. D. Kevan, D. H. Rosenblatt, M. G. Mason, J. G. Tobin, and D. A. Shirley, Phys. Rev. Lett. **45**, 1877 (1980).
[74]Y. Jugnet, F. J. Himpsel, Ph. Avouris, and E. E. Koch, Phys. Rev. Lett. **53**, 198 (1984).
[75]D. Menzel, P. Feulner, R. Treichler, E. Umbach, and W. Wurth, Phys. Scr. **T17**, 166 (1987).
[76]D. Wurth, C. Schneider, E. Umbach, and D. Menzel, Phys. B **34**, 1336 (1986).
[77]G. Loubriel, T. Gustafsson, L. I. Johansson, and S. J. Oh, Phys. Rev. Lett. **49**, 571 (1982).
[78]J. Stöhr, J. L. Gland, W. Eberhardt, D. Outha, R. J. Madix, F. Sette, R. J. Koestner, and U. Doebler, Phys. Rev. Lett. **51**, 2414 (1983).
[79]W. Wurth, C. Schneider, R. Treichler, E. Umbach, and D. Menzel, Phys. Rev. B **35**, 7741 (1987).
[80]B. N. J. Person and Ph. Avouris, J. Chem. Phys. **79**, 5156 (1983); P. Nordlander and Ph. Avouris, J. Vac. Sci. Technol. A **5**, 1099 (1987).
[81]H. Ueba and A. Yoschimori, Surf. Sci. **175**, 659 (1986).
[82](a) D. Lovrić and B. Gumhalter, Phys. Status Solidi B **139**, 423 (1987); (b) D. Lovrić and B. Gumhalter (unpublished).
[83](a) K. Wandelt, J. Vac. Sci. Technol. A **2**, 802 (1984); (b) K. Wandelt and J. E. Hulse, J. Chem. Phys. **80**, 1340 (1984); (c) R. J. Behm, C. R. Brundle and K. Wandelt, J. Chem. Phys. **85**, 1061 (1986).
[84]J. W. Gadzuk, Phys. Rev. B **14**, 2267 (1976).
[85]F. J. Himpsel (unpublished).
[86]F. J. Himpsel, Y. Jugnet, D. E. Eastman, J. J. Donelon, D. Grimm, G. Landgren, A. Marx, J. F. Morar, C. Oden, R. A. Pollack, and J. Schneir, Nucl. Instrum. Methods **222**, 107 (1984).